TECHNICAL REPORT

ISO/TR 14999-2

First edition
2005-03-01

Optics and photonics — Interferometric measurement of optical elements and optical systems —

Part 2: Measurement and evaluation techniques

Optique et photonique — Mesurage interférométrique de composants et systèmes optiques —

Partie 2: Mesurage et techniques d'évaluation

Reference number
ISO/TR 14999-2:2005(E)

© ISO 2005

Copyright International Organization for Standardization
Reproduced by IHS under license with ISO
No reproduction or networking permitted without license from IHS

Not for Resale

PDF disclaimer

This PDF file may contain embedded typefaces. In accordance with Adobe's licensing policy, this file may be printed or viewed but shall not be edited unless the typefaces which are embedded are licensed to and installed on the computer performing the editing. In downloading this file, parties accept therein the responsibility of not infringing Adobe's licensing policy. The ISO Central Secretariat accepts no liability in this area.

Adobe is a trademark of Adobe Systems Incorporated.

Details of the software products used to create this PDF file can be found in the General Info relative to the file; the PDF-creation parameters were optimized for printing. Every care has been taken to ensure that the file is suitable for use by ISO member bodies. In the unlikely event that a problem relating to it is found, please inform the Central Secretariat at the address given below.

© ISO 2005

All rights reserved. Unless otherwise specified, no part of this publication may be reproduced or utilized in any form or by any means, electronic or mechanical, including photocopying and microfilm, without permission in writing from either ISO at the address below or ISO's member body in the country of the requester.

ISO copyright office
Case postale 56 • CH-1211 Geneva 20
Tel. + 41 22 749 01 11
Fax + 41 22 749 09 47
E-mail copyright@iso.org
Web www.iso.org

Published in Switzerland

--`,,`,,,,-`-`,,`,,`,`,,`---

Copyright International Organization for Standardization
Reproduced by IHS under license with ISO
No reproduction or networking permitted without license from IHS

Not for Resale

© ISO 2005 – All rights reserved

Contents

Page

Foreword ... iv

Introduction ... v

1 Scope ... 1

2 Measurement objects ... 1
2.1 Surfaces ... 1
2.2 Optical components in transmission ... 2
2.3 Optical systems ... 3
2.4 Indirect examination of the function of optical elements ... 3

3 Hardware aspects of an interferometer and test environment ... 4
3.1 General ... 4
3.2 Construction principles and influences on the quality of measurements ... 5
3.3 Test environment ... 15

4 Methods for evaluating the optical path difference ... 18
4.1 General ... 18
4.2 Visual inspection of interferograms ... 18
4.3 Manual evaluation of interferograms ... 24
4.4 Phase measurements with temporal carrier ... 26
4.5 Phase measurements with spatial carrier ... 32
4.6 Removal of phase ambiguities (phase unwrapping) ... 34
4.7 Registration of wavefronts; coordinate systems, coordinate system definition ... 35
4.8 Polynomial and other representations of wavefronts ... 36

5 Test reports and calibration certificates ... 38
5.1 General ... 38
5.2 Content of test reports and calibration certificates ... 39
5.3 Test reports ... 39
5.4 Calibration certificates ... 39
5.5 Opinions and interpretations ... 40
5.6 Electronic transmission of results ... 40
5.7 Format of reports and certificates ... 40
5.8 Amendments to test reports and calibration certificates ... 41

6 Data format ... 41

Annex A (informative) **Orthogonal polynomials** ... 42

Annex B (informative) **Orthogonal functions on "unusual areas"** ... 56

Bibliography ... 59

© ISO 2005 – All rights reserved

Copyright International Organization for Standardization
Reproduced by IHS under license with ISO
No reproduction or networking permitted without license from IHS
Not for Resale

Foreword

ISO (the International Organization for Standardization) is a worldwide federation of national standards bodies (ISO member bodies). The work of preparing International Standards is normally carried out through ISO technical committees. Each member body interested in a subject for which a technical committee has been established has the right to be represented on that committee. International organizations, governmental and non-governmental, in liaison with ISO, also take part in the work. ISO collaborates closely with the International Electrotechnical Commission (IEC) on all matters of electrotechnical standardization.

International Standards are drafted in accordance with the rules given in the ISO/IEC Directives, Part 2.

The main task of technical committees is to prepare International Standards. Draft International Standards adopted by the technical committees are circulated to the member bodies for voting. Publication as an International Standard requires approval by at least 75 % of the member bodies casting a vote.

In exceptional circumstances, when a technical committee has collected data of a different kind from that which is normally published as an International Standard ("state of the art", for example), it may decide by a simple majority vote of its participating members to publish a Technical Report. A Technical Report is entirely informative in nature and does not have to be reviewed until the data it provides are considered to be no longer valid or useful.

Attention is drawn to the possibility that some of the elements of this document may be the subject of patent rights. ISO shall not be held responsible for identifying any or all such patent rights.

ISO/TR 14999-2 was prepared by Technical Committee ISO/TC 172, *Optics and photonics*, Subcommittee SC 1, *Fundamental standards*.

ISO 14999 consists of the following parts, under the general title *Optics and photonics — Interferometric measurement of optical elements and optical systems*:

— *Part 1: Terms, definitions and fundamental relationships* (Technical Report)

— *Part 2: Measurement and evaluation techniques* (Technical Report)

— *Part 3: Calibration and validation of interferometric test equipment* (Technical Report)

— *Part 4: Interpretation and evaluation of tolerances specified by ISO 10110*

© ISO 2005 – All rights reserved
Copyright International Organization for Standardization
Reproduced by IHS under license with ISO
No reproduction or networking permitted without license from IHS
Not for Resale

Introduction

A series of International Standards on *Indications in technical drawings for the representation of optical elements and optical systems* has been prepared by ISO/TC 172/SC 1, and published as ISO 10110 under the title *Optics and photonics — Preparation of drawings for optical elements and systems*. When drafting this standards series and especially its Part 5, *Surface form tolerances* and Part 14, *Wavefront deformation tolerance*, it became evident to the experts involved that additional complementary documentation is required to describe how the necessary information on the conformance of the fabricated parts with the stated tolerances can be demonstrated. Therefore, the responsible ISO Committee ISO/TC 172/SC 1 decided to prepare an ISO Technical Report on *Interferometric measurement of optical wavefronts and surface form of optical elements*.

When discussing the topics which had to be included into or excluded from such a Technical Report, it was envisaged that it might be the first time, where an ISO Technical Report or Standard is prepared which deals with wave-optics, i.e. that is based more in the field of physical optics than in the field of geometrical optics. As a consequence only fewer references than usual were available, which made the task more difficult.

Envisaging the situation, that the topic of interferometry has so far been left blank in ISO, it was the natural wish to now be as comprehensive as possible. Therefore there was discussion, whether important techniques such as interference microscopy (for characterizing the micro-roughness of optical parts), shearing interferometry (e.g. for characterizing corrected optical systems), multiple beam interferometry, coherence sensing techniques or phase conjugation techniques should be included or not. Other techniques, which are related to the classical two beam interferometry, like holographic interferometry, Moiré techniques and profilometry were also mentioned as well as Fourier transform spectroscopy or the polarization techniques, which are mainly for microscopic interferometry.

In order to complement ISO 10110 the guideline adopted was to include what presently are common techniques used for the purpose of characterizing the quality of optical parts. Decision was made to complete a first Technical Report, and to then up-date it by supplementing new parts, as required. It is very likely that more material will be added in the near future as more stringent tolerances (two orders of magnitude) for optical parts and optical systems become mandatory when dealing with optics for the EUV range (wavelength range 6 nm to 13 nm) for microlithography. Also, testing optics with EUV radiation (the same wavelength as they are later used, e.g. at-wavelength testing) can be a new challenge, and is not covered by any current standards.

This part of ISO 14999 should cover the need for qualifying optical parts and complete systems regarding the wavefront error produced by them. Such errors have a distribution over the spatial frequency scale; in this part of ISO 14999 only the low- and mid-frequency parts of this error-spectrum are covered, not the very high end of the spectrum. These high-frequency errors can be measured only by microscopy, measurement of the scattered light or by non-optical probing of the surface.

A similar statement can be made regarding the wavelength range of the radiation used for testing. ISO 14999 considers test methods with visible light as the typical case. In some cases, infrared radiation from CO_2-lasers in the range of 10,6 µm is used for testing rough surfaces after grinding or ultraviolet radiation from excimer-lasers in the range of 193 nm or 248 nm is used for at-wavelength testing of microlithography optics. However, these are still rare cases, which are included in standards, that will not be dealt with in detail. The wavelength range outside these borders is not covered.

--`,,```,,,,````-`-`,,`,,`,`,,`---

© ISO 2005 – All rights reserved

Copyright International Organization for Standardization
Reproduced by IHS under license with ISO
No reproduction or networking permitted without license from IHS
Not for Resale

--`,,`,,`,,,-`-`,,`,,`,`,,`---

Copyright International Organization for Standardization
Reproduced by IHS under license with ISO
No reproduction or networking permitted without license from IHS

Not for Resale

Optics and photonics — Interferometric measurement of optical elements and optical systems —

Part 2: Measurement and evaluation techniques

1 Scope

This part of ISO 14999 gives fundamental explanations to interferometric measurement objects, describes hardware aspects of interferometers and evaluation methods, and gives recommendations for test reports and calibration certificates.

2 Measurement objects

2.1 Surfaces

2.1.1 Mirrors: boundary surfaces of optical components in transmission

A common task in interferometry is measurement of the shape of a surface. This can be accomplished in two different ways. Either reflected light or the light transmitted through the surface could be used for the measurement.

Interferometric measurement is achieved by comparing the difference of two optical path lengths $\int nd$. Usually one path is called the reference path, the other the measurement path.

The resulting wave aberration, ΔW, for a displacement d of the surface, if measured in reflection, is $\Delta W = 2nd$. The same displacement measured in transmission results in the wave aberration $\Delta W = \left(n_2 - n_1\right)d$.

2.1.2 Reflection degree

The Fresnel reflection from the boundary between two different media, R, can be calculated from the refractive index n_1 and n_2 at the boundary surface.

$$R = \left(\frac{n_2 - n_1}{n_2 + n_1}\right)^2 \tag{1}$$

For most optical glasses this value is between 4 % and 6 %, so an average of 5 % is usually a good estimate.

This reflection causes a loss of light from the transmitted wavefront at every surface. On the other hand, this reflection is often used for the measurement itself. To obtain maximum fringe visibility, or contrast, the two interfering beams should have approximately the same intensity. Changing the reflectivity of the beam splitter within an interferometer only changes the amount of light in the interference pattern and does not change the beam intensity ratio of the two beams because the light in both arms is transmitted through and reflected by the beam splitter once. If the measurement path and reference path are separated, as in a Mach-Zehnder or Twyman-Green set-up, it is usually possible to adjust the intensities of the light in both arms.

© ISO 2005 – All rights reserved

Copyright International Organization for Standardization
Reproduced by IHS under license with ISO
No reproduction or networking permitted without license from IHS
Not for Resale

A major problem arises in a Fizeau interferometer. If the reference surface has high reflectance, the result will be multiple beam interference fringes resulting in narrow fringes as in a Fabry-Perot interferometer. If sinusoidal fringes are required as for the evaluation by phase shift interferometry, the reference surface shall have low reflection and an element has to be introduced between the reference and the measurement surface that will absorb light without distorting the wave aberration.

2.1.3 Roughness

For interferometric measurement the roughness of the measured surface should not exceed a certain limit that is a fraction of the wavelength and of the difference of indices of refraction, if used in transmission.

2.1.4 Topology of the regions

Difficulties may arise with interferometer software when the wavefront area has breaks in it (e.g. because it is split into segments by the mechanical supports of the secondary mirror of a mirror telescope). Problems are most severe with static fringe analysis software that depends strongly on using neighbouring points to determine the position and continuity of fringes. Phase shift software is not affected to the same extent as it is a point-by-point evaluation of wave aberrations.

Similar problems may occur if the wavefront area has a complicated outline.

2.1.5 Continuity of the surface; gradient of the surface

Due to the inherent ambiguity of $\pm n \cdot 2\pi$ it is not possible to measure any arbitrary surface shape uniquely. The evaluation of a surface is usually correct, if the wave aberration between two resolvable points is less than π.

The gradient of the surface under test relative to the reference surface results in a gradient of the measured wave aberration and in high-density or closely spaced fringes. Interferograms cannot be evaluated, if the fringe separation is less then twice the distance of two resolvable points. If this condition is not possible by adjustment, or by changing the measurement set-up, compensating optics may be required in some cases.

Some of the problems caused by the ambiguity can be solved by multiple wavelength interferometry.

2.1.6 Stiffness of mirrors; finite-element-calculations

During measurement the method of supporting the optics being tested should not deform them other than when used as intended. It is sometimes difficult to notice whether an object is deformed during the measurement. As a first indication of the influence of the support, the object can be measured by supporting it in two completely different ways. In the case of any doubt, a finite-element-calculation is recommended.

2.1.7 Temperature homogeneity of mirrors

During measurement the object shall have a homogeneous temperature. Inhomogeneous temperatures can cause deformations as the expansion coefficient of optical materials is rather high and the thermal conductivity is very low. Stabilization can take some minutes but may sometimes require several hours.

2.1.8 Examples of measurement objects

Items that can be measured by interferometry include optical flats, windows, raw glass, convex and concave mirrors, lenses, prisms, and optical systems.

2.2 Optical components in transmission

2.2.1 Single-pass versus double-pass testing

Transmitting optical components can be measured in single-pass or double-pass, depending on the interferometric set-up. Double-pass measurement increases the sensitivity by a factor of two but may also

© ISO 2005 – All rights reserved
Copyright International Organization for Standardization
Reproduced by IHS under license with ISO
No reproduction or networking permitted without license from IHS
Not for Resale

include the effect of the reflecting surface. In double-pass measurements consideration shall also be given to the possibility that the returning light passes back through the component at different locations.

2.2.2 Windows (wavefront aberrations in transmission)

For windows the shape error of the surfaces is usually not important. Also, the measured transmitted wavefront will include the homogeneity of the material. Depending on the application, a certain amount of power may be tolerated separate from the other wave aberrations. Also, a tolerated wedge can be measured by interferometry. However, it can be more convenient to measure angular errors by different equipment.

2.2.3 Prisms (wavefront aberrations and angle error)

As in the case for windows, the wave aberrations and angular errors of prisms can be measured by different equipment. However, if the angular tolerances are in the interferometric region, and many parts are to be measured, it can be more convenient to measure both features by interferometry. In this case a fixed set-up, or a master specimen, is used as a reference.

2.2.4 Influence of temperature on the refractive index

For measurement of an optical component in transmission, it shall be noted that not only the objects might be deformed by the thermal expansion but, also, that the refractive index of the material changes with temperature. Therefore, thermal setting of the test piece before testing is even more important.

2.3 Optical systems

2.3.1 Single-pass versus double-pass testing

Complete optical systems can be measured by interferometry in a manner similar to the testing of single components. It is, however, important that systems be measured in the same geometry as they were designed to be used. This can lead to a complicated set-up in single or double pass. For long systems tested in double pass and in the presence of severe aberrations, it is necessary to take into account that the light path on the way back can be considerably different to that in the forward direction.

2.3.2 Examination in the pupil

Interferometric measurements should be made in the exit pupil of the optical system.

2.3.3 Chromatic aberrations

If systems are measured at wavelengths different than those they are designed for, the effects caused by chromatic aberrations shall be computed. There will be some systems, where the wave aberrations can be simply scaled by the ratio of the test and design wavelengths, whereas other systems are so different that a measurement is not possible.

2.4 Indirect examination of the function of optical elements

2.4.1 Examination with different wavelength

Usually the measurement of windows is possible and can be scaled to the correct wavelength. It shall be noted, however, that inhomogeneities of optical materials may to some degree depend on the wavelength range. Because of the presence of chromatic aberrations no universal recommendation is possible.

2.4.2 Examination with different beam path

Usually the measurement set-up should be as similar as possible to the application. In some cases, however, it is more convenient to measure optical elements in a way that is different from their use. In this case, it may

--`,,`,,,-`-`,,`,,`,`,,`---

© ISO 2005 – All rights reserved

Copyright International Organization for Standardization
Reproduced by IHS under license with ISO
No reproduction or networking permitted without license from IHS
Not for Resale

be difficult to find a correlation between the measured wave aberration and the tolerances and, therefore, not possible to evaluate how the application is affected.

2.4.3 Tolerance range

Sometimes the relationship between the interferometric measurement and the tolerances of the measured objects is not clear. Usually the complete test set-up shall be considered.

3 Hardware aspects of an interferometer and test environment

3.1 General

The purpose of this clause is to acquaint the user of an interferometer set-up to possible influences on the accuracy of measurements. It is a matter of fact that two different persons using the same hardware and doing their measurements in the same laboratory, will not necessarily achieve identical results with their measurements. The skilled user might achieve a highly accurate result, whereas the unskilled user might have severe errors in his result that he might not be aware of. It is important to keep in mind that good reproducibility of measurement is no guarantee for a correct result, because systematic sources of errors might have influenced the measured results. Knowledge about such possible influences, and how to avoid them, is what experimental skill is about.

Such sources of errors can be, for example:

— improper use of the measuring instrument, because the optical principles are not well understood, e.g. failure to image the surface under test onto the CCD camera of the interferometer;

— use of unsuitable fixtures to hold the test piece, inducing strain which causes bending;

— influence of gravity on the test piece;

— vibrations of the test set-up, which might induce phase-measuring errors;

— unsuitable use of polynomial fits with respect to the given shape of the aperture (for example due to some obscured parts of the circular shape) and adjacent subtraction of error terms like tilt and focus terms, due to an violation of the orthogonality assumption;

— presence of stable layers of air with different temperatures in the interferometer cavity, causing coma and astigmatism;

— flipping (mirroring), or some other mismatch, of a calibration error map with respect to the actual orientation, shape or magnification of the measured field;

— influence of different temperature or different focus settings between calibration and measurement;

— use of test pieces which are not homogeneous in temperature and have a considerable coefficient of temperature expansion.

These are only examples; although there are a much greater number of “typical” sources of error. The only way to overcome such types of error, which depend very much on the actual test situation and the demands for the final accuracy, is that the operator planning and assembling the test should be aware of possible influences on the accuracy of the measurement, which might be of optical or mechanical nature.

Conceptually, it is very important not to believe blindly the results which the instrument shows. At the same time, it is equally important not to blame the instrument, or the principle of the interferometric measurement, if there are inexplicable results. Note that in the majority of cases the instrument shows the “correct” readings from what is presented to it, even if that is not the measurement task in question. If, for example, the measured error map does not rotate by 72° when the test piece is rotated physically by 72°, this might indicate

© ISO 2005 – All rights reserved
Copyright International Organization for Standardization
Reproduced by IHS under license with ISO
No reproduction or networking permitted without license from IHS
Not for Resale

that the reference surface may contribute a considerable amount to the total error. The support of the test piece can also influence the measurement, etc.

Another test might be, to repeat the measurement after 1 h without touching anything in the meantime. If the results deviate from each other the reason might be that the temperature of the supports of the surface under test, may have had an uneven temperature distribution in the first test. Normally, it may take more than 30 min before the temperature has homogenized after handling a part. Also, the temperature in the laboratory might have changed, the instrument might have warmed up, etc.

Such tests are imperative in order to exclude at least the most common sources of error. It is strongly recommended to repeat a measurement at least three times and compare the results; this repetition should include the demounting and remounting of the part in the test set-up, as well as all the adjustments of the set-up and the settings of the interferometer. It is even better to repeat the whole test procedure on another day, and, even by another operator.

All measurement conditions and settings have to be documented and the final data sets should be stored in the computer in an organized way. Ideally, the documentation should be stored together with the measured data sets. Any further treatment like subtraction of tilt or even higher order (Zernike) functions, number of averages, any filtering like smoothing with a spatial low pass or median filter to remove “spikes”, shall be documented and stored together with the data set. Such information is part of the result and when not given together with the measured surface map, the result is useless and cannot be used for proof of quality for the part under test.

3.2 Construction principles and influences on the quality of measurements

3.2.1 General

When the wavefront deviation of a test piece is measured by an interferometer, the test piece becomes part of the optics of the instrument. The auto-collimation condition shall be met, as well as the condition to image the surface under test onto the detector. In order to achieve high flexibility of possible locations for the surface under test and for different test configurations, there will be stringent requirements on the spatial and temporal coherence of the light source which need to be fulfilled. These can easily be attained by use of a laser and, together with a very high intensity compared to other light sources, are the reason that the laser is the standard light source for interferometers.

One of the consequences of the very high coherence of lasers is that all kinds of defects, such as impurities of substrates, optical cements and coatings, tiny scratches, bubbles, holes, dust particles, micro-roughness of surfaces, which can occur at any part of the light path through the interferometer, are “collected” and are superimposed as an uncleanliness, i.e. unwanted amplitude and phase modulations of the wavefronts which finally show clearly on the interferogram. The further away the disturbing defects are from an image plane of the detector, the more the defects are altered in their phase distributions due to Fresnel diffraction and in spatial frequency. A very narrow defect located on a surface near an image of the light source might spread out to a big size in the detector plane. The specification of optical parts used in an interferometer set-up therefore have to be much more stringent than in conventional optical instruments and depend on the position of the part in the ray-path. For surfaces which are at a position near the image of the light source, where the diameters of the ray bundles are small, ultra-high surface quality requirements shall be fulfilled. Generally speaking, the higher the test accuracy has to be, the more severe are the demands for the quality of all parts.

As discussed in ISO/TR 14999-1, it is very important to image the wavefront under test onto the detector plane. If the location of this wavefront relative to the instrument changes from one test set-up to another, a possibility of refocusing the detector to this new location shall be provided. In some instruments, provision is made to alter the magnification with which the wavefront under test is imaged onto the detector. In some cases, this is done in fixed steps, in other cases this is done continuously over a certain range. On the other hand, it is necessary to attain a good optical wavefront-correction when “tailoring” the wavefronts in the instrument to the desired shape and at the same time realizing a good optical transfer function for the amplitude and phase when imaging the wavefront under test at the detector plane.

All such possibilities and demands cause a certain amount of complexity of the optical layout of such an instrument, leading to optical systems with multiple surfaces. It is obvious that it is more difficult to keep the

© ISO 2005 – All rights reserved

Copyright International Organization for Standardization
Reproduced by IHS under license with ISO
No reproduction or networking permitted without license from IHS
Not for Resale

unwanted additional disturbances by the optical parts small when more optical parts are necessary to achieve the desired functionality. The skill of the designer of an instrument lies in finding the best compromise between the degree of aberration correction (keeping the wavefront errors with low spatial frequency small) and the degree of noise (i.e. high spatial frequency errors). The noise increases with every additional surface which might be necessary for aberration correction. Since the complexity of the optical layout grows with the universality of the use of the instrument, it is much easier to construct a high-quality single-purpose instrument.

Due to higher cost of production, and the deterioration in the appearance of the interferograms obvious to any customer, companies tend to minimize the number of optical elements and seek to achieve the best correction for wavefront aberrations. This might have consequences for the handling of the instrument. If, for example, the transmission sphere, used for spherical testing, is not aligned properly when attached to the instrument, coma and astigmatism might be introduced into the measured wavefront. If deviations in the alignment of the focus setting between calibration measurements and final measurements for the parts under test exist, this again might cause wavefront errors in the final results. On the other hand, a highly corrected instrument might be much more “robust” against such higher order errors, but at the cost of a higher number of surfaces and therefore a higher amount of coherent noise.

The opposing criteria for the way to design a laser interferometer require a compromise between wavefront quality, field correction, versatility on the one hand and number and location of surfaces on the other hand.

3.2.2 Intrinsic instrument errors and the principle of common path

The task gets more and more difficult when the errors, which have to be measured accurately, become smaller and smaller. It might be concluded from this that it would be nearly impossible to get reliable measuring results. Needless to say, it is necessary that the “intrinsic errors” caused by the instrument itself should be at least not higher than the errors caused by the test piece. Example: suppose the test piece is a very well polished spherical surface of a lens. The interferometer itself might include in total 12 lens surfaces and another 10 surfaces of plane plates. Therefore, it would be necessary to fabricate the 22 surfaces within the instrument to a degree of perfection that is at least 22 times better than that of the test piece in order to attain the same disturbance from the instrument (i.e. “intrinsic errors”) and from the test piece. Or, if argued with statistically distributed errors, it might be concluded that already a factor 4 to 5 would be sufficient. Even in the latter case, it would be nearly impossible to fabricate and maintain an instrument with such a degree of perfection.

This argument is both right and wrong. It is the principle of interference that errors common to both waves, i.e. the test wave and the reference wave, cancel out. The ultimate use of this principle is apparent in the Fizeau type interferometer, where all but the last surface before the surface to be tested and the air between these two surfaces are common to both waves. The quantity that is measured by a Fizeau interferometer is the optical path difference between the two surfaces facing each other (the “optical thickness-distribution” of the air-gap; this includes the distribution of the refractive index of the air). So far the argument is wrong; but it is right for very small-scale errors. It is never possible for the rays to travel exactly the same path, so the principle of “common path” with cancellation of common errors is always violated, if high spatial frequency noise is in demand. So, even if Fizeau interferometers are more robust for errors with low spatial frequencies, this is not the case for coherent noise.

In order to check the sensitivity of an instrument to alignment errors as well as for intrinsic high frequency noise, the following two tests can be useful.

a) The following simple test should be repeated with different orientations of the fringes and also with the highest number of fringes the instrument is capable of measuring. This test is one measure for the robustness of the instrument against misalignments of all kinds. Proceed as follows.

   1) Place a reference flat in front of the transmission flat of the instrument and adjust for about 25 fringes of tilt.

   2) Perform a measurement and store the result.

   3) Adjust for zero-fringes and perform another measurement.

© ISO 2005 – All rights reserved
Copyright International Organization for Standardization
Reproduced by IHS under license with ISO
No reproduction or networking permitted without license from IHS
Not for Resale

4) Subtract both data sets and compute the Zernike terms for the resulting difference-data set; besides other errors, the induced wavefront tilt with respect to the optical axis make visible the optical wavefront aberrations which go along with the small angle of the test wave.

b) The second test checks the intrinsic high frequency noise and therefore the ability to detect small-scale errors which normally go along with very small amplitudes. Proceed as follows.

1) Take the data of the difference from the measurement on-axis and the measurement with the 25 fringes of tilt.

2) Subtract the first 36 Zernike terms. The remaining surface map shows mainly the intrinsic coherent noise of the instrument.

3) When “spikes”, which occur at the boundary of measured part, are removed, the r.m.s. value is a quality number for the intrinsic noise. This noise should be uncorrelated when the experiment is repeated with different orientations of the fringes and therefore reduce with the square root law, if measurements with different fringe orientations are averaged and the difference of those averages are calculated instead of the difference of only two measurements.

Together with these tests, it is recommended that two other simple checks be performed to assess the proper alignment of the instrument:

The collimation of the plane-wave leaving the system can be checked with the help of a thick ($>$ 30 mm) plane-parallel plate of known good optical quality by inserting the plane parallel plate with an incident angle of 45° into the beam and projecting the lateral shearing interferogram onto a screen. If the plate has no wedge-angle, no fringes should be visible, but they will be present if the wavefront from the interferometer converges or diverges.

The adjustment for the alignment reticle, or other means for the alignment of the beam, can also be checked using a corner-cube mirror or prism of known good quality. The returning beam should be incident precisely at the centre of the alignment device. This is also a method for adjusting the reference surface perpendicular to the beam. By tilting the reference surface, the interference fringes formed by the reference wave and a wave reflected by the triple-mirror (having three surfaces with angles of 90° between them) should be made as broad as possible.

3.2.3 Optical compensation of errors

It is a very useful property of two-beam interference that the physical principle can help to suppress the errors caused by component parts of the interferometer. If the two interfering beams experience the same disturbances when passing through the optical parts, the wavefront errors impressed on them are identical and cancel out in the final wavefront difference. Therefore, the two wavefronts should travel almost the same path through the instrument so ensuring that “optical compensation” of errors takes place. This is achieved best by the arrangement of a Fizeau test set-up, where the test surface and the reference surface face each other without any component in between. This cancellation is not necessarily perfect, if there are deviations in the optical path when the beams are tilted with respect to each other.

Another deviation from perfect symmetry of the interfering waves is due to the imaging conditions of the two surfaces in question onto the detector. The two surfaces in a Fizeau configuration, the test surface and the reference surface, cannot both be imaged exactly onto the detector surface at the same time. Normally, the reference surface is larger than necessary, so that the surface under test defines the final aperture for the size of the interferogram. In this case, no errors are introduced to a first order by Fresnel diffraction at the boundary of the reference surface, when this boundary is larger than the diameter used. Nevertheless, there remains an error influence, but it is so small, that it will not be visible in most cases. There is another higher-order error, which will be explained in conjunction with the testing of spherical surfaces with a so-called “Fizeau transmission sphere”.

Figure 1 shows the optical conditions when testing a spherical surface T with respect to a reference surface R. In this example, it is assumed that the reference surface R (this is the last surface of the transmission sphere) as well as the test-surface T are both concave. The apexes of the surfaces are called S_R and S_T. The Fizeau

--`,,`,,,-`-`,,`,,`,`,,`---

© ISO 2005 – All rights reserved

Copyright International Organization for Standardization
Reproduced by IHS under license with ISO
No reproduction or networking permitted without license from IHS
Not for Resale

cavity is set up correctly when both surfaces are arranged so that they have a common centre of curvature. If the Fizeau lens is calculated and manufactured properly, this centre point coincides with the focal point F of the spherical wave, illuminating the reference surface R. It is supposed that this is the case.

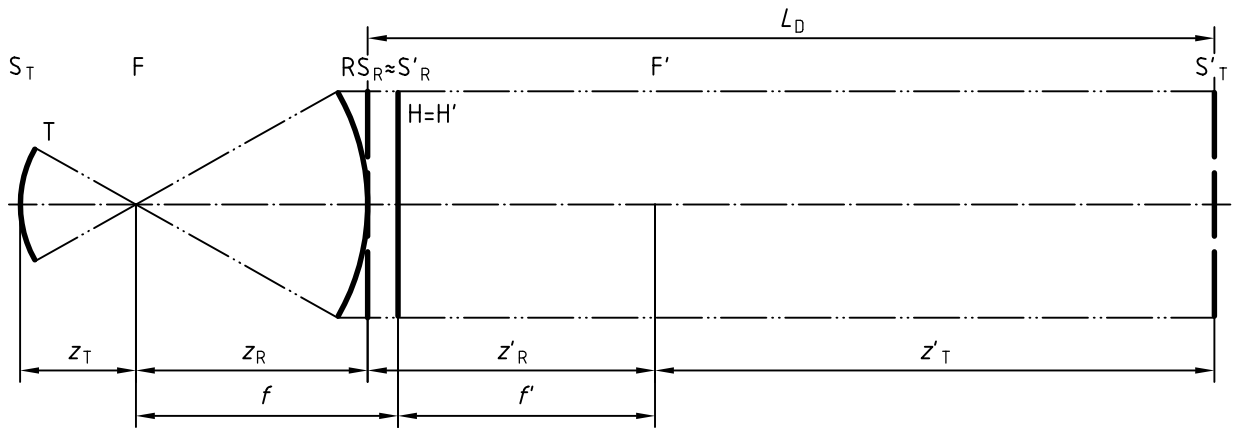

Key

L_D defocus

Figure 1 — The images S_R' and S_T' of the apexes of the reference surface S_R and the test surface S_T are defocused with respect to each other

As can be seen from Figure 1, both surfaces in question are imaged by the transmission sphere (which is optically represented by the principal plane H=H′ and the focal points F and F′) into different locations at the optical axis. The sizes of the images match, but the axial distance between the images, L_D (the "defocus") is shown in Figure 1. Now, it is supposed that there might be aberrations already present in the wavefront illuminating the transmission sphere as well as additional aberrations added by the transmission sphere itself. The transmission sphere should image an infinite object into the focus point F without introducing additional spherical aberration, as well as the test surface T into its image T′ and the reference surface R into R′ without adding different phase-terms into these images.

As was explained in ISO/TR 14999-1:2005, 2.11, only ideal plain waves do not alter their shape when they spread out. So, even if we suppose that the two wavefronts at the locations S_R' and S_T' might still have the same shape, i.e. the same aberrations, the fact that one of them has to travel the distance "defocus" will cause them to deviate from each other when they meet to interfere on the detector. This effect is the more pronounced the larger the distance "defocus" is compared to the diameter of the wavefront. As a rule of thumb, the radius of the test surface should not be smaller than 10 % of the focal length of the transmission sphere. Also, the transmission sphere should not introduce an error greater than $\lambda/2$ in double pass. For high-precision measurements, these tolerances shall even be more stringent.

It is important to keep in mind that any wavefront error, which is already present in the plane wavefront entering the transmission sphere, will be made visible also by this effect of defocused images. There is no way to overcome this problem with Fizeau interferometers other than to keep the defocus as small as possible by using a transmission sphere with the smallest possible air gap. The influence of this error can be minimized by appropriate calibration measurements.

3.2.4 Mathematical compensation of errors

The great advantage of "optical compensation" of errors due to the principle of "common path through the optics" is that this compensation takes place in "real time", i.e. continuously during the measurement.

In contrast to that approach, an even better effect can be gained when two measurements are performed, including all the errors of a test set-up "left over" by the optical compensation scheme (Fizeau or Twyman-Green or others). The first measurement is with a "calibration master" and the second with the test piece. The resulting error maps are stored in computer memory. Suppose that nothing but the master and test pieces

© ISO 2005 – All rights reserved
Copyright International Organization for Standardization
Reproduced by IHS under license with ISO
No reproduction or networking permitted without license from IHS
Not for Resale

have changed between the measurements, the difference of the two measurements should show only the difference in the shape of the master piece and the test piece. All other errors should cancel out by this "mathematical compensation for the intrinsic errors" of the test set-up. Therefore the master plays a similar role as the reference wavefront, but this time some higher order errors, like "defocus" discussed in the context with Figure 1, also cancel out due to the higher degree of "symmetry" compared to the normal Fizeau test.

The drawback with this method is that, in principle, two measurements are necessary to get the result which increases the statistical errors by a factor of $\sqrt{2}$, and that the two measurements cannot be performed both at the same time. In order that this mathematical compensation of errors be effective, it shall be assured that the calibration measurement is still valid for the actual measurement of the test piece. It is therefore highly recommended to take the calibration measurement at a time immediately before or after (or both) the measurement of the test surface.

This "mathematical compensation" can have some important advantages compared to the "optical compensation":

— Master piece and test piece may have the same radius of curvature, e.g. the imaging properties onto the detector are identical both times.

— Influences of gravitational deformations, quasi-stationary temperature gradients, etc., are cancelled out to some extent.

— The reference piece may be made much thicker than the transmission sphere will normally be. If it is made more stable than the test piece, this might be helpful in some situations. For example, the "bending" of the test piece by the support will show in the result. In other cases, it may be possible to produce an almost identical master (but with a known error map) for calibration purposes.

— A greater flexibility exists for the design of the test configuration. Especially, the reference surface does not have to be the last surface of a transmission sphere any longer, but it could be a plane surface in front of the lens. In this way, "tilt" can be introduced into the test configuration, without causing uncompensated errors.

This last point is an important one, and will be explained later in greater detail.

3.2.5 Contrast as a function of the irradiance in test and reference arm: methods to attain equilibrium in both arms

It is well known (see ISO/TR 14999-1:2005, 3.2.1), that the intensity of two beam interference $I(x)$ is described by the formula

$$I(x) = I_1(x) + I_2(x) + 2\sqrt{I_1(x)I_2(x)}\,|\gamma|\cos\left[\frac{2\pi}{\lambda}\Delta l_{\mathrm{OPD}}(x)\right] \tag{2}$$

where

x is a vector describing the spatial coordinates, which may be on the detector or the surface under test;

Δl_{OPD} is the complete "optical path difference" of the two interfering beams, in principle from the light source all the way down to the detector (practically, in Fizeau interferometers, it is twice the "optical thickness" of the cavity, because of the (quasi) identical paths of the two beams through most parts of the interferometer, as was discussed before);

$|\gamma|$ is the magnitude of the complex degree of coherence; this quantity is close to unity in most cases when using a laser as the light source;

$I_1(x)$ and $I_2(x)$ are the intensities of the interfering wavefronts when measured separately.

--`,,```,,,-`-`,,`,,`,`,,`---
© ISO 2005 – All rights reserved
Copyright International Organization for Standardization
Reproduced by IHS under license with ISO
No reproduction or networking permitted without license from IHS
Not for Resale

The visibility V of the fringes is given by

$$V = \frac{2\sqrt{I_1 \cdot I_2}}{I_1 + I_2}|\gamma| \tag{3}$$

If we assume that $|\gamma|$ = 1, then the visibility can be expressed as a function of the relative magnitude of the intensities of the two waves, e.g. as a function of

$$\eta = \frac{I_2}{I_1} \text{ with } I_2 \leqslant I_1 \tag{4}$$

Then, the visibility is

$$V = \frac{2\sqrt{I_1 I_2}}{I_1 + I_2} = \frac{2\sqrt{\frac{I_2}{I_1}}}{1 + \frac{I_2}{I_1}} = \frac{2\sqrt{\eta}}{1+\eta} \qquad \text{for} \qquad 0 \leqslant \eta \leqslant 1 \tag{5}$$

Figure 2 gives the function $V = V(\eta)$. Table 1 provides related values.

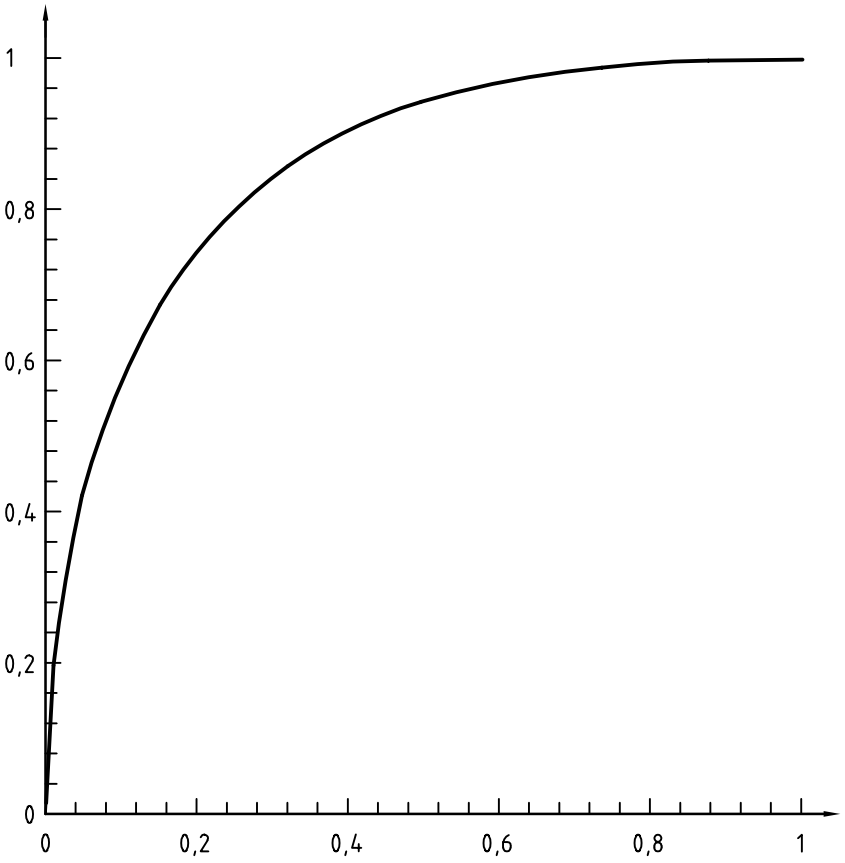

Figure 2 — Visibility of two-beam interference as a function of the ratio $\eta = I_1 / I_2$ of the intensities of the two waves

© ISO 2005 – All rights reserved
Copyright International Organization for Standardization
Reproduced by IHS under license with ISO
No reproduction or networking permitted without license from IHS
Not for Resale

Table 1 — Intensities I_1, I_2, intensity-ratio η, visibility V and number of bits lost, when the intensities of the two-beam interference are not equal

I_1	I_2	η	V	bit		I_1	I_2	η	V	bit
1	1	1,000	1,00	0,00		1	1,00	1,000	1,00	0,00
2	1	0,500	0,94	0,08		1	0,90	0,900	1,00	0,00
5	1	0,200	0,75	0,42		1	0,80	0,800	0,99	0,01
10	1	0,100	0,57	0,80		1	0,50	0,500	0,94	0,08
20	1	0,050	0,43	1,23		1	0,10	0,100	0,57	0,80
25	1	0,040	0,38	1,38		1	0,06	0,060	0,46	1,11
50	1	0,020	0,28	1,85		1	0,04	0,040	0,38	1,38
100	1	0,010	0,20	2,34		1	0,03	0,030	0,34	1,57
200	1	0,005	0,14	2,83		1	0,02	0,020	0,28	1,85
400	1	0,003	0,10	3,33		1	0,01	0,010	0,20	2,34

It can be seen from Table 1 that the visibility drops to 38 % of its optimal value, when the intensities differ by a factor of 25, e.g. when a highly reflective test surface is measured against an uncoated Fizeau reference plate. In the case where the evaluation of the phase map is made by a phase-measuring technique and the intensities are measured by a CCD camera, this is equivalent to a degradation of the contrast by 1,38 bits. If the camera in the interferometer has a quantization into only 8 bits, which is the case in most systems, this might degrade the measurement precision unacceptably, whereas with cameras of 10 bits or 12 bits of quantization, the degradation might be acceptable. In any case, this effect can be compensated by raising the number of measurements to be included in one average by a factor of $N = 1 / V^2 = (1 + \eta)^2 / 4\eta$, which is approximately seven in our example.

If this is not adequate, it will be necessary to adjust the intensities in the two beams, i.e. attenuate the reflectance of the higher reflecting surface. Possible ways to achieve this are discussed for two versions of a Twyman-Green configuration as well as for a Fizeau configuration. In the Twyman-Green configurations it is assumed that the beam splitter BS has no absorption and that the reflectance of the test-surface T and the reference surface R are ρ_T and ρ_R respectively. The absorbance for the attenuator is abbreviated by α_A. η is the abbreviation for the ratio of the reflectances ρ_R / ρ_T.

The possible interferometer configurations are given in Figure 3.

--`,,`,,,--`,,`,,`,`,,`---

© ISO 2005 – All rights reserved

Copyright International Organization for Standardization
Reproduced by IHS under license with ISO
No reproduction or networking permitted without license from IHS
Not for Resale

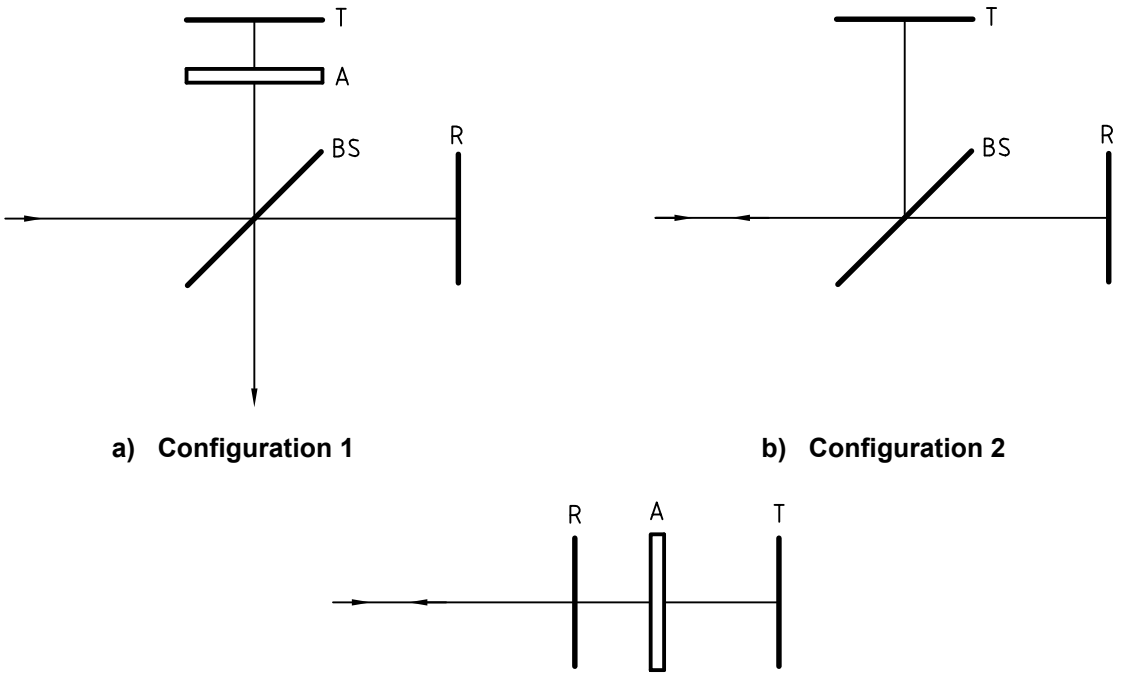

a) Configuration 1

b) Configuration 2

c) Configuration 3

The necessary attenuations and reflectance and transmittance values for the beam splitter are:

a) Configuration 1 $\alpha_A = \sqrt{\frac{\rho_R}{\rho_T}} = \sqrt{\eta}$

b) Configuration 2

$$\begin{cases} \rho_{BS} = \dfrac{\sqrt{\rho_T \rho_R} - \rho_R}{\rho_T - \rho_R} = \dfrac{\sqrt{\eta} - \eta}{1 - \eta} \\ \tau_{BS} = \dfrac{\rho_T - \sqrt{\rho_T \rho_R}}{\rho_T - \rho_R} = \dfrac{1 - \sqrt{\eta}}{1 - \eta} \\ \text{with} \quad \eta = \dfrac{\rho_R}{\rho_T} \text{ and with } \rho_T \geqslant \rho_R \end{cases}$$

c) Configuration 3 $\alpha_A = \sqrt{\frac{\rho_R}{\rho_T}} = \sqrt{\eta}$

In the Fizeau configuration, the reflectance of the reference surface should not be higher than 4 %, to avoid the influence of multiple-reflections on the fringe-profile.

Figure 3 — Three configurations with unequal reflectance for the test surface T and the reference surface R

In the Twyman–Green configurations, only a pure two-beam interference will take place, whereas the Fizeau configuration suffers from the fact that multiple reflections within the cavity will occur. This effect can be neglected in most cases, provided that the reflectance of the reference surface (the so-called “transmission flat”) is no greater than 4 %. For very high precision measurements, the true shape of the fringes should be taken into account for the evaluation formula used for phase-measuring analysis.

The attenuator plate A in Figure 3 should be of very high quality; normally an absorbing coating is applied onto a plane parallel plate made of fused silica or BK7. From Figure 3, it is clear that the attenuator plate A is an

© ISO 2005 – All rights reserved
Copyright International Organization for Standardization
Reproduced by IHS under license with ISO
No reproduction or networking permitted without license from IHS
Not for Resale

integral part of the cavity, and the influence of this plate (double transmission) to the transmitted wavefront will be part of the measured result, adding to the errors of the test piece. If it is possible to use the “empty cavity”, the change in the measured wavefront as a result of the insertion of the attenuator can very easily be determined. Thus, it is possible to mathematically correct for the influence of the attenuator.

3.2.6 Contrast as a function of performance of the light source

3.2.6.1 General

The generalized interferometer may be considered as composed of:

— an optical source,

— a collimating device,

— the interferometric device,

— a focusing device, and

— a detector.

The light emitted by the optical source is used to generate interference patterns and the detector collects the information, i.e. the interferogram.

Interferogram contrast depends on the following parameters:

a) spectral domain,

b) coherence, and

c) polarization of the light.

The light source has to be chosen in accordance with the application.

3.2.6.2 Spectral domain

3.2.6.2.1 Source and detector

The user will choose the source to match its spectral emission range and the spectral sensitivity of the detector. The emission range should be close to the maximum sensitivity.

NOTE In the case of visual observation, a green (filtered mercury lamp) or a yellow source (sodium spectral lamp for close to null path difference) are the best choice (they correspond to the peak eye sensitivity); a red laser diode can be a poor choice for colour-defective observers.

3.2.6.2.2 Factors impacting transmission and reflection

Between the source and the detector, light will be subject to transmissions and/or reflections when travelling through the collimating, interferometric and focusing devices. These devices can distort the initial spectral emission range of the light passing through them.

NOTE For example, a gold-coated mirror has a poor reflectance in the blue and green spectral range; the reflectance increases in the yellow spectral range and is high in the red and infrared spectral ranges. With a silver coating, the reflection curve peaks in the yellow spectral range. With an aluminium coating, the visible spectral range is not affected.

Therefore, care shall be taken when selecting the source.

© ISO 2005 – All rights reserved

Copyright International Organization for Standardization
Reproduced by IHS under license with ISO
No reproduction or networking permitted without license from IHS
Not for Resale

3.2.6.2.3 Control requirements

If the sample is to be used with a pre-determined wavelength, the user has less freedom in the choice of source and detector, and will operate with the required wavelength. In some cases, the use of a substitute wavelength is possible, but in this case appropriate information about this shall be included in the test report.

3.2.6.3 Temporal coherence

3.2.6.3.1 Pragmatic representation

Whatever the theoretical approach to describing the temporal coherence of the light, an elementary approach is to consider the beam as a light wave train. The train is limited in length equivalent to the coherence length.

The light wave train will travel from the source to the detector. Reaching the beam-splitter, the train is divided into two “subtrains”, one going through the reference arm, and the other through the measurement arm of the interferometric device. After their separate paths, both subtrains reach the component used for the light wave train reconstruction (the beam-splitter in some cases). The reconstructing optical component performs an addition of both subtrains, equal to the initial light wave train, if possible. The subtrains are fully superposed if the arm lengths are equal, or one subtrain is delayed if its arm is longer than the other one.

The interference contrast is maximum when the arm-lengths are equal, but decreases as they become unequal.

NOTE The contrast obtained with a helium-neon laser decreases when the path difference is in the range of centimetres (the coherence length is usually considered to be in the range of the laser mechanical length).

The contrast obtained with a medium price laser diode is very poor, when the path difference is in the range of centimetres, and periodically re-appears and disappears, when the path difference increases. This is due to the multi-ray emission of the laser diode.

The contrast obtained with a Na spectral lamp oscillates as the path difference varies, the period corresponds to a path difference of 0,6 mm due to the Na doublet.

The contrast obtained with a Hg low-pressure spectral lamp goes to zero, when the path difference becomes close to one centimetre.

The coherence obtained with a Hg high-pressure spectral lamp decreases very rapidly as the lamp temperature goes up, and is quickly reduced to less than one millimetre. Nevertheless, the user can maintain a longer coherence length by using a rheostat in the lamp power supply to cool the lamp during operation.

3.2.6.3.2 Sample surface contribution

The user has to consider the question “Is the source coherence compatible with the roughness (peak-to-valley) of the test piece?” although it is rare to be limited by the coherence when observing the defects (peak-to-valley) of a test piece.

On the other hand, it is important to adapt the form of the comparison wavefront to the surface of the sample. This means, the user will adapt the shape of the wavefront to the sample shape, the goal being to keep the variations of path difference lower than the source coherence at all points.

NOTE For example, the way to measure the quality of an aspheric surface is to give the wavefront the radius of the best sphere, where the best sphere is the one which minimizes the distances to the surface when incident on the sample.

3.2.6.3.3 Sample thickness contribution

When the measurement beam has to travel through the test piece, two effects have to be considered.

© ISO 2005 – All rights reserved
Copyright International Organization for Standardization
Reproduced by IHS under license with ISO
No reproduction or networking permitted without license from IHS
Not for Resale

First, is the delay given to the “subtrain” going through the sample arm. Consider a sample with a thickness T and a refractive index n. It will introduce in the measurement arm a path difference of $2(n - 1)T$. This path difference can be compensated by moving the mirror of the reference arm away from the beam-splitter.

Secondly, the sample can be considered as a thick window plate with parallel faces. This window plate gives an image from the mirror of the sample arm, translated from its initial position. The translation is $(n - 1)T/n$ in the direction or the beam-splitter.

In total, the user wants to extend the reference arm, and the sample reduces the length of the measurement arm. The user has to place the reference mirror in a compromise position, taking the coherence and the fringe visibility into account.

3.3 Test environment

3.3.1 General

The ideal interferometer system would be a system delivering the same correct results in any environment, independent of vibrations, temperature and temperature gradients, gravity and distribution of forces supporting the test piece. Such a “magic” interferometer could be thought of as having the ability to act as a filter, which completely blocks all environmental influences. At the same time, it would be completely responsive to all the surface form information of the test surface, sensing this to the highest precision, which might be in the range of sub-nanometres normally to the surface and more than 1 million measured points in the most demanding cases. Also, such an ideal instrument would not contribute any intrinsic errors or noise to the measurements.

In practice, it is impossible to block all environmental influences and intrinsic errors or noise by the instrument. But, still, there are a number of ways that a designer of an instrument can make it more (or less) robust against environmental influences.

It is also evident that the influence of the environment can be kept constant by keeping the environment itself constant. In a laboratory equipped with high grade air-conditioning, shielding against vibrations, acoustic noise, very stable and noise-free voltage supply, etc., and, ideally, if the tests were performed in a zero-gravity environment, it would be much easier to attain reproducible results. The quality of the laboratory environmental conditions will influence the precision of the result, but not necessarily accuracy; hence, generally the importance of a very good laboratory is overestimated.

However, besides the laboratory and the instrument, there is a third influence: the operator of the instrument. In most practical cases, the instrument and the laboratory will already be provided, and the operator will thus be the key-person to influence the ultimate accuracy and precision within the given limitations.

3.3.2 Influence of vibrations

When testing optical surfaces, e.g. using a Fizeau interferometer as given in Figure 14 of ISO/TR 14999-1:2005, the two interfering waves are reflected back from the last surface V as well as the reference surface M. These two surfaces have to be mounted and this mount has to provide the necessary stability. It is essential to ensure that the gap between the surfaces will not change unintentionally during the acquisition of the intensity data in a (conventional) phase-measurement approach with temporal carrier as described in 4.4.

The reason for this is, that in the case of an additional change of the “interferometer cavity” due to vibrations of the mount carrying the parts, Equation (8) is no longer complete since $\varphi(t)$ now contains not only the wanted term as described in 4.4, but also an unwanted component describing the vibrations in the cavity. This “noise” term, φ_N, can, in the simplest case, be described by Equation (6).

$$\varphi_N = 2\left(\frac{2\pi}{\lambda}\right) a \sin \omega_N t \tag{6}$$

© ISO 2005 – All rights reserved

Copyright International Organization for Standardization
Reproduced by IHS under license with ISO
No reproduction or networking permitted without license from IHS
Not for Resale

where

a is the amplitude of the vibration;

ω_N is the (dominant) frequency.

Even if the noise might contain a complicated spectrum, in many cases it will be sufficient to restrict the consideration to one single frequency with the lowest mechanical eigenfrequency ω_N of the structure and the largest associated amplitude a.

Given specific phase algorithm and given the frequency of the camera frames, it is possible to compute the amount of the phase errors due to a, under the assumption that a is small enough (on the order of $\lambda/10$) that the linear model can be applied. There are significant differences between the phase algorithms.

As interferometry can be used to measure deviations of wavefronts or surfaces as small as a few nanometres or even smaller, it is obvious that the test pieces need to be mounted in a stable manner. It is therefore common practice to install the interferometer on a passive or even better actively-controlled vibration isolated table, which acts as a low-pass filter to the vibrations of the floor of the laboratory. If possible, there should be no running machines in the vicinity of the laboratory.

However, many circumstances exist where it is difficult to avoid sources of vibrations or to isolate well enough. In this case, it is useful to investigate the result of vibrations on the measurements in order to optimize the given set-up or, in addition to the vibration isolation, to apply further means to minimize the effects of vibrations. For example, this could be an electronic stabilization of the interferometer cavity using a high speed camera in conjunction with a powerful laser and a “two-step” phase algorithm, or the use of phase measurement algorithms which are not sensitive to unwanted and unknown phase shifts between several camera frames. Two groups of algorithms can be distinguished here:

— phase-measurement algorithms with spatial carrier frequency (see 4.5), and

— algorithms which do not require *a priori* knowledge of the phase steps.

The latter approach is especially interesting in cases where already reasonably good starting values for the phase steps can be assured, which are then further refined in an iterative optimization process, i.e. when the vibration isolation is already very good but still the remaining disturbance is too high for the application. The phase steps are taken here as additional unknowns which need to be determined in addition to the phase values. Note, that only the phase values are functions of the spatial coordinates but are not time dependent, whereas the phase-step between two adjacent camera frames is one single time-dependent quantity.

It is very important for the user of a phase-measuring interferometer to know how to check the set-up for vibrations which might degrade the result. For a better understanding of the procedure described hereafter, it is useful to state that the phase-errors $\Delta\phi(x,y)$ due to vibrations can be expressed by:

$$\Delta\phi(x,y) = \varepsilon \sin\left[2\phi(x,y)\right] + \ldots \text{small higher order terms} \tag{7}$$

where the amplitude ε of the sine function is dependent on a number of parameters as:

— the specific algorithm used;

— the amplitude of the vibration;

— the ratio of the dominant vibration frequency ω_N to the camera frame frequency ω_0, i.e. ω_N/ω_0;

— the exposure time of the camera.

It is interesting that the dominant error term in square brackets [ ] has as its argument twice the phase value to be measured, i.e. $2\phi\ (x,y)$. Therefore, to decide whether ε is small enough to be ignored, the following procedure is useful:

© ISO 2005 – All rights reserved
Copyright International Organization for Standardization
Reproduced by IHS under license with ISO
No reproduction or networking permitted without license from IHS
Not for Resale

a) introduce fringes into the interferogram by tilting the object;

b) compensate for piston only and count the number of “fringes” in the result after phase shift measurement and calculation.

If it is twice the number of the pre-set fringes in the interferogram, then ε is not small enough.

3.3.3 Influence of gravity and support of the test piece

The effect of the support of the test piece on the measuring result under the influence of gravity shall be taken into consideration.

For many practical cases, the effect is quantitatively foreseeable by mathematical means. For practically edited details, see for example Reference [4]. Such an analysis is often a rather complicated procedure, which consists in solving differential equations or in FEM calculations. Fortunately, a detailed mathematical analysis is required only in cases where the highest measuring accuracy is required.

Some basic facts and rules of thumb are very useful to estimate the magnitude and help to avoid considerable measuring errors.

a) Optical materials vary in their stiffness by a factor of 10 (see Table 2). Optical glass BK7 has its place in the geometrical middle between the extrema. The sag varies between three times to one third of the value for BK7.

b) From mechanics it is known that the sag of a twofold supported beam (or straight-edge) is minimized if the support points are arranged at nearly one fifth of the beam length away from the beam ends (the so-called minimum deflection points separated by 0,55 length). This rule is useful if a horizontally arranged standard surface is to be optimally supported.

c) Table 2 shows some numerical values for the sag of uniformly loaded (gravity) circular plates supported continuously around their edges. It shows the effect of different materials (A in Table 2), thickness according to the common rule “D/d = 8” (B in Table 2), and the required thickness to result in a constant sag of 33 nm (C in Table 2).

Table 2 — Sag of uniformly loaded circular plates

Effect	Material	Diameter mm	Thickness mm	Sag nm
A	LF5	120	10	48,3
	SF59	120	10	108,6
	Saphir	120	10	10,5
	BK7	120	10	27,4
B	BK7	20	2,5	0,3
	BK7	60	7,5	3,0
	BK7	120	15	12,2
	BK7	200	25	33,9
	BK7	300	40	66,9
	BK7	400	50	135,4
C	BK7	400	100	33,9
	BK7	300	55	35,4
	BK7	200	25	33,9
	BK7	120	9	33,9
	BK7	60	2,3	32,4
	BK7	20	0,25	33,9

© ISO 2005 – All rights reserved

Copyright International Organization for Standardization
Reproduced by IHS under license with ISO
No reproduction or networking permitted without license from IHS
Not for Resale

4 Methods for evaluating the optical path difference

4.1 General

Various procedures exist for the accomplishment of interferometric measurements. This clause provides an overview of them, together with information-associated errors from random and systematic sources, as well as certain specific procedures for high-accuracy measurements.

The various methods for the evaluation of interferograms can be divided into the following.

a) Visual or manual procedures giving qualitative information about shape of the test wavefront (or surface) and simple characteristic values (e.g. PV value).

b) Phase measuring procedures yielding a complete quantitative description of the wavefront (or surface) under test.

4.2 Visual inspection of interferograms

4.2.1 General

An interferogram arises from a comparison of a test wavefront (surface) with a known reference wavefront (surface). The shape and orientation of the reference wavefront should be adequately chosen, so that the ideal test wavefront leads to a typical interference pattern (e.g. straight fringes) which is easy to interpret.

By observing the deviation of the actual interferogram from this ideal pattern, the various optical aberrations of wavefronts, as well as typical wavefront and surface distortions can be recognized and classified by their visual appearance.

In addition, it is important to gain information about the sign of the wavefront aberration, i.e. whether the distortion is a peak or a valley, or whether a test wavefront (surface) is convex or concave with respect to a reference wavefront (surface). This phase information is not contained in a static interference pattern or interferogram. To obtain it, it is necessary to ascertain and record the location of the zero order of the interference pattern, i.e. the location where the optical path difference between the interfering wavefronts is zero. Knowing the location of the zero order, and applying a variation of the optical path difference in a known way, it is possible to deduce the sign of the wavefront (surface) deviation by observation of the direction of motion of the fringes:

— If the optical path difference is decreased, the fringes move away from the direction of the zero order (for tilted wavefronts: to the thick portion of the wedge).

— If the optical path difference is increased, the fringes move toward the direction of the zero order (for tilted wavefronts: to the thin portion of the wedge).

— If the tilt between the wavefronts is increased, the fringe spacing is decreased and the fringes move toward the zero order fringe.

If possible, the interferometer should be adjusted “with tilt”, so that the path difference contains an air wedge to obtain nearly straight fringes.

4.2.2 Example 1 — Fizeau interferometer

A hole will cause fringes to move toward the thin portion of the air wedge (Figure 4).

© ISO 2005 – All rights reserved
Copyright International Organization for Standardization
Reproduced by IHS under license with ISO
No reproduction or networking permitted without license from IHS
Not for Resale

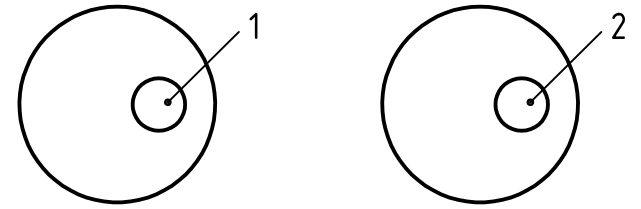

a) Top view

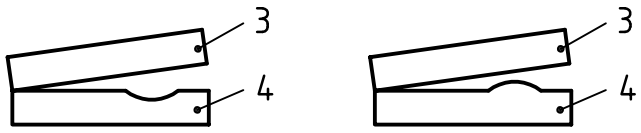

b) Side view

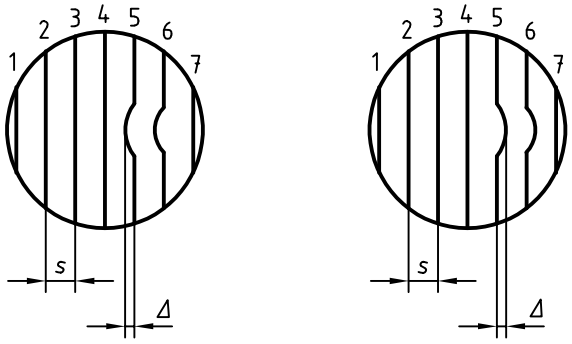

c) Interferogram

Key

1 hole
2 bump
3 reference surface
4 test surface

S fringe spacing in the best-fitting pattern
Δ maximum of the fringe pattern from the best-fitting pattern

Figure 4 — Movement of fringes in case of a hole and a bump, respectively

For a concave surface, the fringes at the edge of the pattern curve toward the thick portion of the wedge; for a convex surface the fringes curve toward the thin portion of the air wedge (Figure 5).

© ISO 2005 – All rights reserved

Copyright International Organization for Standardization
Reproduced by IHS under license with ISO
No reproduction or networking permitted without license from IHS
Not for Resale

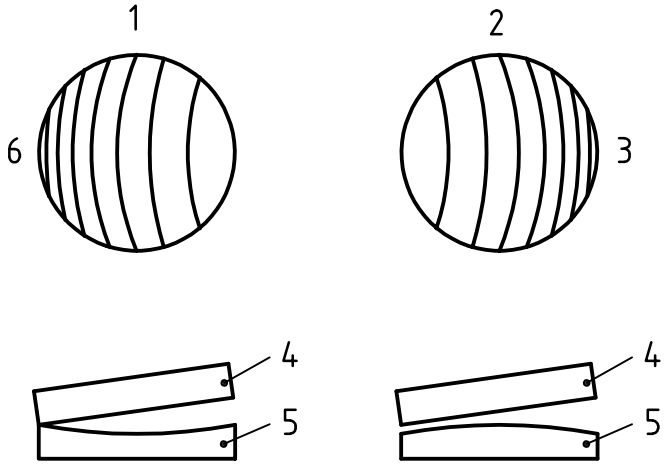

Key

1 concave sphere
2 convex sphere
3 thick part of wedge
4 reference flat
5 test surface
6 thin part of wedge

Figure 5 — Movement of fringes in case of a concave and a convex surface, respectively

Figure 5 assumes that the wedge angle between the two wavefronts being compared is larger than the wavefront errors, and thus no closed fringes are obtained. The wedge angles in the drawings are greatly exaggerated.

If the wedge direction is not known, it can be determined as described in Table 3.

For the general case, where the fringes are neither circular nor straight, a combination of these facts apply. Firstly, the direction of the zero order as described for straight fringes has to be determined. Secondly, the direction the fringes curve relative to the zero order has to be observed to determine whether the wavefront/surface is convex or concave. This also applies to local distortions.

In the case of spherical wavefronts or surfaces, the sign of the optical path difference, Δl_{OPD}, indicates that the test wavefront is either concave or convex relative to the reference wavefront, which is important in the fabrication of optical surfaces as well as in the assembly of optical systems. Table 3 also contains the determination of the relative curvatures of test and reference surface (wavefront) in a wedge-free set-up (e.g. proof glass). If the test surface is convex relative to the reference surface, a decrease in air gap thickness causes the fringes to move out, away from the zero order [see Figure 6 a)]. In this case, the radius of curvature of the test surface is longer than the radius of the reference surface. If on the other hand, the test surface is concave relative to the reference surface, a decrease in air gap thickness causes the fringes to move in, i.e. away from the zero order, and the radius of curvature of the test surface is shorter than the radius of the reference surface [Figure 6 b)].

In these considerations, the expression “surface” may be exchanged by “wavefront”.

© ISO 2005 – All rights reserved
Copyright International Organization for Standardization
Reproduced by IHS under license with ISO
No reproduction or networking permitted without license from IHS
Not for Resale

Table 3 —Determination of the sign of defect for a Fizeau interferogram

a) Interferometer set-up with tilt (containing air wedge)	
Wedge direction known	
Hole	Fringe deviation from straightness toward thin portion of wedge
Bump	Fringe deviation from straightness toward thick portion of wedge
Concave sphere	Fringes curve toward thick portion of wedge
Convex sphere	Fringes curve toward thin portion of wedge
Wedge direction not known	
— Push on edge of test piece to determine direction of wedge	
Number of fringes increase: pushing on thin portion of wedge	
Number of fringes decrease: pushing on thick portion of wedge	
— Pushing uniformly on test piece to decrease air gap thickness	
Closed fringes: fringes move toward low points	
Open fringes: fringes move from higher regions to lower regions	
— Pushing uniformly on test piece to increase air gap thickness	
Closed fringes: fringes move toward high points	
Open fringes: fringes move from lower regions to higher regions	
b) Interferometer set-up without tilt (air wedge), comparing spherical surfaces	
Test wavefront (surface) radius > reference radius	
— When decreasing air gap thickness: fringes move out, away from the zero order	
— Fringes are curved towards the zero order	
— Wavefront (surface) convex to reference	
Test wavefront (surface) radius < reference radius	
— When decreasing air gap thickness: fringes move in, away from the zero order	
— Fringes are curved away from the zero order	
— Wavefront (surface) concave to reference	

--`,,`,,,`-`-`,,`,,`,`,,`---

© ISO 2005 – All rights reserved

Copyright International Organization for Standardization
Reproduced by IHS under license with ISO
No reproduction or networking permitted without license from IHS
Not for Resale

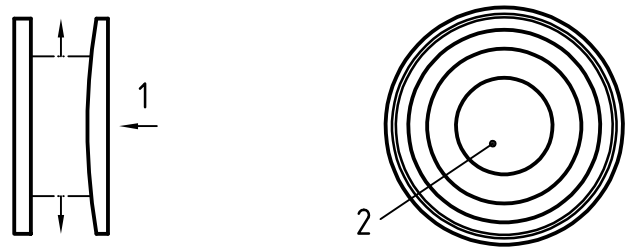

a) Fringes move out

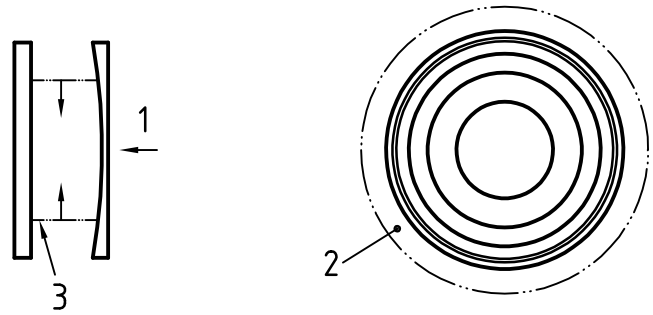

b) Fringes move in

Key

1 push
2 zero order
3 constant distance corresponding to fringe

Figure 6 — Fringe movement

© ISO 2005 – All rights reserved
Copyright International Organization for Standardization
Reproduced by IHS under license with ISO
No reproduction or networking permitted without license from IHS
Not for Resale

4.2.3 Example 2 — Twyman-Green interferometer

Table 4 outlines several common techniques for determining the sign of the error.

Table 4 — Determination of the sign of defect for a Twyman-Green interferogram

a)	**Push in on reference mirror** 1) Closed fringes — Surface test: fringes move toward high points — Transmission test: fringes move toward thin regions 2) Open fringes — Surface test: fringes move from low regions to high regions — Transmission test: fringes move from thick regions to thin regions
b)	**Push out on reference mirror** Opposite of 1
c)	**Push in on test mirror** Opposite of 1
d)	**Push out on test mirror** Same as 1
e)	**Put hot wire in test beam** 1) Closed fringes — Surface test: in vicinity of the wire fringes move toward lower regions — Transmission test: in vicinity of the wire fringes move toward thick regions 2) Open fringes — Surface test: in vicinity of the wire fringes move from high regions to low regions — Transmission test: in vicinity of the wire fringes move from thin regions to thick regions
f)	**Put hot wire in reference beam** 1) Closed fringes: opposite of 5 a) 2) Open fringes: opposite of 5 b)

Note that a change in spacing without a change in relative tilt between the wavefronts is nearly impossible to achieve.

When testing optical systems, the visual inspection of the interferogram allows (for simple cases and small aberrations) a rough statement about the nature of the aberration. Some typical cases are illustrated in Figures 7 and 8.

© ISO 2005 – All rights reserved

Copyright International Organization for Standardization
Reproduced by IHS under license with ISO
No reproduction or networking permitted without license from IHS
Not for Resale

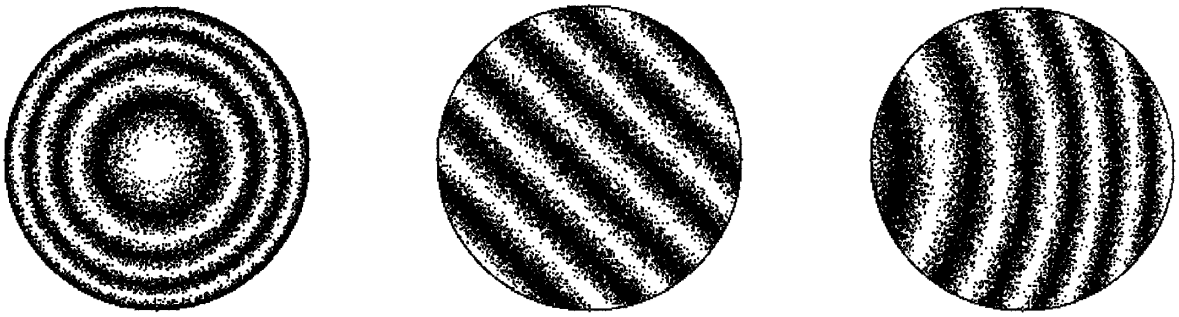

a) Pure defocus b) Pure tilt c) Defocus + tilt

Interferograms show adjustment of interferometer.

Figure 7 — Interferograms for a system under test without small aberrations

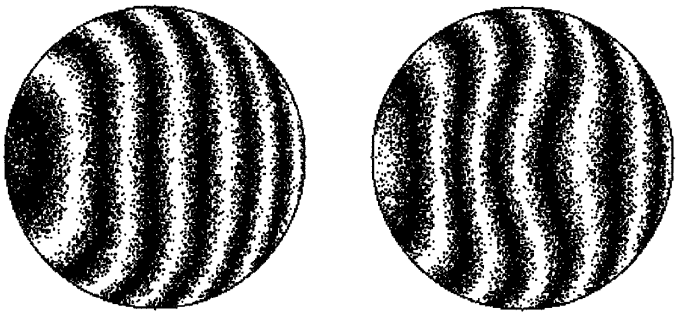

a) Spherical aberration

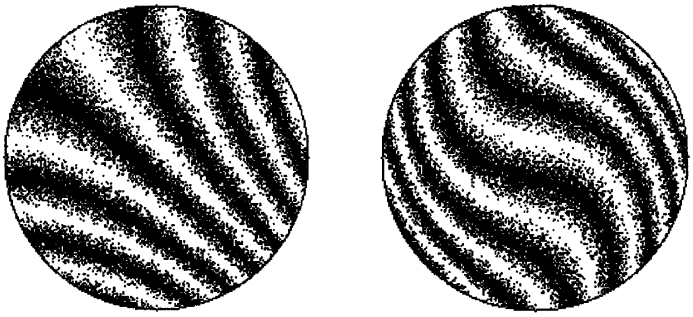

b) Astigmatism c) Coma

Interferograms additionally show typical aberration-dependent patterns.

Figure 8 — Interferograms for a system under test with small aberrations

4.3 Manual evaluation of interferograms

To evaluate an interference fringe pattern, it is necessary to quantify the deviation of the fringe pattern from some ideal best-fitting pattern, which is expected for some specific (best-fitting) test wavefront. Depending on this theoretical wavefront, several kinds of deviations can be extracted from the interferogram, i.e. wavefront sagitta error, irregularity and rotationally symmetric irregularity (see ISO 10110-5:1996, Annex B). Ideally, the fit should be based on a least-squares computation.

© ISO 2005 – All rights reserved
Copyright International Organization for Standardization
Reproduced by IHS under license with ISO
No reproduction or networking permitted without license from IHS
Not for Resale

In practice, try to adjust for straight fringes (minimum sagitta error), so that the estimation, respectively manual evaluation, can be done with the help of a ruler or specially designed hinged mechanical parallelogram. If this is not possible (e.g. when using proof glasses), the central fringe should not be compared to a straight line, but to the circular arc joining the two ends and the centre of the central fringe.

The deviation, denoted distortion, is usually presented as a fraction of the spacing between a pair of fringes in the ideal pattern. See Figure 9.

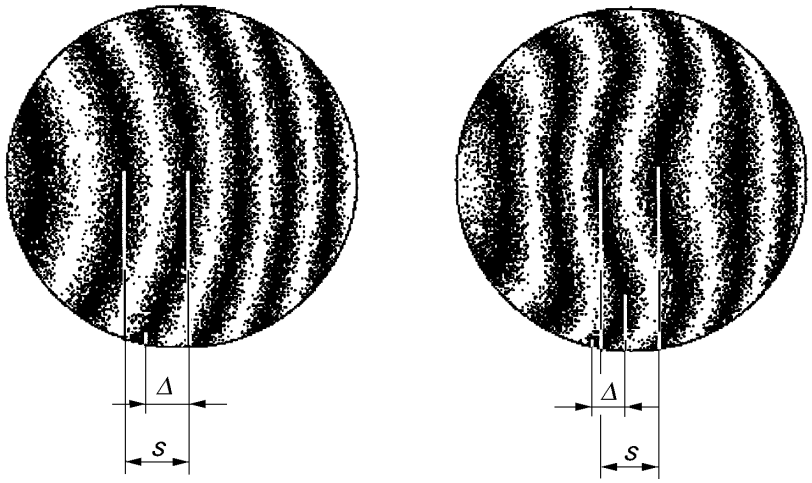

Key

S fringe spacing in the best-fitting pattern

Δ maximum of the fringe patern from the best-fitting pattern

Figure 9 — Manual evaluation of interferograms

Quantitatively, Δ/s is the fractional distortion in the fringe spacing, where s is the fringe spacing in the best-fitting pattern, and Δ is the maximum deviation of the fringe pattern from the best-fitting pattern. This corresponds to the maximum distance between the test and reference wavefront minus the minimum distance between the wavefronts. In this case, where the wavefronts intersect, the minimum distance between the wavefronts is a negative number; the sign shall be taken into account in computing the difference, which is called the peak-to-valley (PV) difference. If one of the wavefronts represents the theoretical planar wavefront, then the peak-to-valley difference between the wavefronts is called the “peak-to-valley deformation”.

The distortion, in units of wavelengths, is equal to the product of Δ/s and the “interferogram scale factor”.

$$\text{Distortion} = (\Delta/s) \times (\text{interferogram scale factor}) \times \lambda$$

For example, when evaluating a mirror surface at normal incidence in a Fizeau or Twyman-Green interferometer, the scale factor is 1/2: one fringe spacing = (λ/2).

© ISO 2005 – All rights reserved

Copyright International Organization for Standardization
Reproduced by IHS under license with ISO
No reproduction or networking permitted without license from IHS
Not for Resale

Table 5 gives the interferogram scale factors for some common interferometric set-ups.

Table 5 — Interferogram scale factors

Measured parameter	Interferometric set-up	Interferogram scale factor
Reflective surface	Normal incidence, single pass	1/2
Reflective surface	Angle of incidence = Θ, single pass	$1/(2\cos\Theta)$
Reflective surface	Normal incidence, double pass	1/4
Reflective surface	Angle of incidence = Θ, double pass	$1/(4\cos\Theta)$
Single pass transmitted wavefront distortion	Single pass	1
Single pass transmitted wavefront distortion	Double pass	1/2
Double pass transmitted wavefront distortion	Single pass	2
Double pass transmitted wavefront distortion	Double pass	1

When characterizing a surface form deviation in units of fringe spacings, the word “fringe spacing” does not refer to the transverse distance between fringes, but to the fact that the number of fringe spacings visible in the interference pattern corresponds to the number of half-wavelengths of surface form deviation.

The transmitted wavefront quality of an optical element is judged by the deformation of a planar wavefront transmitted twice through that element. This deformation is measured along the direction of propagation, that is, perpendicular to the nominal plane of the wavefront. The unit of measure is also a “double-pass fringe spacing”, and it is equal to one wavelength of the light.

The r.m.s. measures of wavefront distortion cannot be determined by visual inspection or this elementary manual evaluation.

The analysis of fringe patterns is treated more fully in many textbooks, such as Reference [5].

4.4 Phase measurements with temporal carrier

4.4.1 General

The basic procedures for the analytical evaluation of interference patterns are described in 4.4.2 to 4.4.4, which use a temporally varying reference phase $\varphi(t)$ to measure the phase $\Phi(x,y)$ of the wavefront under test (without sign and phase ambiguity). The description is restricted to the most common case of two-beam interferometry.

The intensity $I(x,y)$ of the interference pattern, recorded on a uniform rectangular grid, obeys the following equation (see ISO/TR 14999-1:2005, 3.1.1):

$$I(x,y) = I_0(x,y)\left\{1 + V(x,y)\cos\left[\Phi(x,y) - \varphi(t)\right]\right\} \tag{8}$$

where

$I_0(x,y)$ is the nearly uniform background intensity;

$V(x,y)$ is the visibility (contrast) of the fringes;

$\Phi(x,y)$ is the phase distribution to be measured;

$\varphi(t)$ is the reference phase.

--`,,```,,,-`-`,,`,,`,`,,`---
© ISO 2005 – All rights reserved
Copyright International Organization for Standardization
Reproduced by IHS under license with ISO
No reproduction or networking permitted without license from IHS
Not for Resale

Since there are three unknowns in the interference equation (I_0, V, Φ), a minimum of three intensity measurements for each location (x,y) is necessary to determine the phase $\Phi(x,y)$.

It is assumed that the relative orientation of both test and reference wavefront is such that the difference $\Delta\Phi$ between neighbouring points on the grid does not exceed π, so there are at least two detector locations for each fringe (sampling according to the Nyquist frequency). Contrary to the manual evaluation methods, no other requirements exist for the relative adjustment of the wavefronts, since in the quantitative description of the test wavefront, tilt and defocus effects can be subtracted.

The temporal modulation of the reference phase is accomplished by continuously or stepwise changing the optical path of one of the interferometer arms. Among various possible devices, the most common are:

— moving reference mirror [mounted on a piezoelectrically driven transducer (PZT)];

— tilted glass plate;

— moving grating;

— rotating polarizers in conjunction with a polarizing dependent interferometer set-up;

— acousto-optical modulator.

These devices are used to either introduce a phase difference between the beams in discrete steps, or to vary the phase difference continuously, which corresponds to a frequency shift.

Depending on the phase variation, several methods can be distinguished (see References [6] and [7]):

— heterodyne interferometry ($\varphi = \omega t$);

— phase lock interferometry ($\varphi = a\sin\omega t + \varphi_0$);

— phase stepping and phase shifting interferometry [$\varphi = (r - 1)\varphi_0$].

NOTE The method described in 4.3 uses a spatially varying phase shift $\varphi = p_0 + p_1 x$, corresponding to a tilt between reference and test wavefront to produce wedge-type straight fringes of a certain spatial frequency. More sophisticated methods relying on spatial phase variation are described in 4.5.

4.4.2 Heterodyne interferometry

The phase difference ($\varphi = \omega t = 2\Delta f t$) between the interfering beams is varied by means of a continuous phase modulator, such as a rotating radial grating, acousto-optic modulator or rotating birefringent device. Since a continuously increasing phase difference corresponds to a second frequency, it is also possible to use a 2-frequency laser. The modulated fringe intensity is photoelectrically detected. At each location (x,y) of the interference pattern, the detector measures a signal at the beat frequency Δf, provided its bandwidth is high enough. The phase measurement can then be performed electronically by comparing two such signals.

One possibility is to use a detector at rest at the location (x_0,y_0) and another detector which is scanned over the whole interference pattern. For each position (x,y) of the scanning detector the phase difference $\Delta\Phi = \Phi(x,y) - \Phi(x_0,y_0)$ is determined by an electronic phasemeter. By integrating these differences over the whole interference pattern, the optical phase difference between the wavefronts can be measured without modulo-2π -ambiguity and including the sign information.

Another possibility is to use a second detector seeing the interference of light beams which are uninfluenced by the probe. The phase of this detector signal is fixed and serves as a reference in the electronic phase measuring.

© ISO 2005 – All rights reserved

Copyright International Organization for Standardization
Reproduced by IHS under license with ISO
No reproduction or networking permitted without license from IHS
Not for Resale

4.4.3 Phase lock interferometry (PLI)

In phase lock interferometry, the phase difference between the interfering beams is modulated sinusoidally with an additional adjustable phase offset φ_0:

$$\varphi(x,y,t) = a\sin\omega t + \varphi_0(x,y,t) \tag{9}$$

A simple possibility to achieve this is a piezoelectrically driven reference mirror. The resulting intensity detected by a photoelectric sensor is

$$I(x,y,t) = I_0\left\{1 + V\cos\left[\Phi(x,y) - \varphi_0(t) - a\sin\omega t\right]\right\} \tag{10}$$

The equation for the interference intensity $I(t)$ at a given position (x,y) contains terms of the type $\cos[a\sin(\omega t)]$ and $\sin[a\sin(\omega t)]$. These terms can be expanded into a series with Bessel functions as coefficients:

$$\begin{aligned} I_{xy}(t) = {} & I_0 + I_0 V\cos(\Phi - \varphi_0)\left\{J_0(a) + 2J_2(a)\cos(2\omega t) + \ldots\right\} \\ & - I_0 V\sin(\Phi - \varphi_0)\left\{2J_1(a)\sin(\omega t) + 2J_3(a)\sin(3\omega t) + \ldots\right\} - \end{aligned} \tag{11}$$

The frequency spectrum of the detected signal U contains components U_0, U_ω, $U_{2\omega}$, ... at the multiples of the modulation frequency ω. For small modulation amplitudes a, these components are:

$$U_\omega \approx I_0 V a\sin(\omega t)\cdot\sin(\Phi - \varphi_0) \tag{12}$$

$$U_{2\omega} \approx \frac{1}{4} I_0 V a^2\cos(2\omega t)\cdot\cos(\Phi - \varphi_0) \tag{13}$$

The signal component U_ω vanishes at the locations of a fringe maximum or minimum, whereas $U_{2\omega}$ reaches a maximum value:

$$U_\omega = 0\,;\; U_{2\omega} = \text{ max.} \tag{14}$$

U_ω can be separated by a suitable electronic filter. With a phase sensitive detector, the offset phase φ_0 can be steered in such a way that $U_\omega = 0$ is locked. So the change of Φ with varying positions (x,y) of the scanning detector is monitored by a variation of φ_0, since the electronic circuit maintains the condition $\varphi_0 = \Phi$.

The main features of this type of interferometry are as follows.

a) The phase detection is very sensitive to phase shifts of the whole apparatus during the scanning procedure; the achievable r.m.s. accuracies are practically limited to $\lambda/30$.

b) The scanning region shall be determined beforehand (with some type of interactive software) to avoid an interruption of the phase tracking if the rim of the interferometric aperture is crossed.

4.4.4 Synchronous detection and phase-shifting interferometry

4.4.4.1 General

Since the interference equation [see Equation (8)] contains three unknowns (I_0, V, Φ), a minimum of three discrete intensity measurements for each location (x,y) in the interference pattern is necessary to determine the phase $\Phi(x,y)$. For more than three measurements the technique corresponds to a least squares fitting procedure with enhanced accuracy.

© ISO 2005 – All rights reserved
Copyright International Organization for Standardization
Reproduced by IHS under license with ISO
No reproduction or networking permitted without license from IHS
Not for Resale

The phase difference between the two beams has to be stepped, preferably the reference phase is shifted such that R measurements are equally spaced over one or more modulation periods:

$$\varphi_r = \frac{(r-1)\,2\pi}{R} \text{ with } r = 1, \ldots, R \tag{15}$$

To solve the resulting equation system, the interference equation [Equation (8)] is rewritten in the following form:

$$I(x,y) = L + M\cos\varphi + N\sin\varphi \tag{16}$$

where

$L = I_0$

$M = I_0 V\cos\Phi$

$N = I_0 V\sin\Phi$ multiplied by $\cos\varphi_r$ respectively $\sin\varphi_r$ and summed up over one period,

where

$\varphi_r = (r-1)\cdot\varphi_0$ and $r = 1, \ldots, R$,

It follows:

$$M \propto \sum_{r=1}^{R} I_r\cos\varphi_r, \qquad N \propto \sum_{r=1}^{R} I_r\sin\varphi_r \tag{17}$$

where I_r being the intensity value belonging to the reference phase value φ_r.

The following equation for the phase Φ holds:

$$\Phi(x,y) = \arctan\frac{N}{M} = \arctan\frac{\sum_r I_r(x,y)\sin\varphi_r}{\sum_r I_r(x,y)\cos\varphi_r} \qquad (\text{mod } \pi) \tag{18}$$

The multiplication with $\sin\varphi_r$ and $\cos\varphi_r$ corresponds to a synchronous detection of the cosine type signal $I_r(\varphi_r)$.

Depending on the actual number of phase steps, there are several common schemes.

4.4.4.2 Four-step technique

With $\varphi_r = 0, \pi/2, \pi, 3\pi/2$, Equation (3) simplifies to:

$$\Phi(x,y) = \arctan\frac{I_2(x,y) - I_4(x,y)}{I_1(x,y) - I_3(x,y)} \tag{19}$$

The fringe visibility can be written:

$$V(x,y) = \frac{\sqrt{(I_1 - I_2)^2 + (I_1 - I_3)^2}}{2I_0} \tag{20}$$

© ISO 2005 – All rights reserved

Copyright International Organization for Standardization
Reproduced by IHS under license with ISO
No reproduction or networking permitted without license from IHS
Not for Resale

For each detector element, the value $V(x,y)$ gives information whether the phase measurement $\Phi(x,y)$ is reliable or not. In an automated measuring procedure it can be used for the determination of the rim of the interference aperture or detection of dust particles, which do not exhibit the sinusoidal φ_r-dependence. If the phase is integrated over $\Delta = \frac{1}{2}\pi$ (four-bucket technique, see 4.4.4.3), the fringe visibility is 0,9 V_{step}.

4.4.4.3 Four-bucket technique

Concerning the measurement time, the phase stepping technique is not the fastest possible procedure, because the phase stepper (for instance a piezo-driven mirror) requires a certain time to settle down after each step. In a modified scheme the phase is shifted continuously during the detector's integration time. The phase change φ_r is divided into R sections in which the relative phase changes by an amount $\Delta = 2\pi/R$. For each section the integrated intensity is:

$$I_r(x,y) = \frac{1}{\Delta}\int_{\varphi_r - \Delta/2}^{\varphi_r + \Delta/2} I_0(x,y)\left\{1 + V\cos\left[\Phi(x,y) - \varphi(t)\right]\right\} d\varphi(t) \tag{21}$$

After integrating this expression, the recorded intensity is:

$$I_r(x,y) = I_0(x,y)\left\{1 + V\,\mathrm{sin}c(\tfrac{1}{2}\Delta)\cos\left[\Phi(x,y) + \varphi_r\right]\right\} \tag{22}$$

where $\mathrm{sin}c(\frac{1}{2}\Delta) = \sin\frac{1}{2}\Delta \big/ \frac{1}{2}\Delta$

So the only difference of this method to phase stepping is a reduction in the detected fringe modulation. In the description of the various phase stepping schemes, this reduction factor will also be given.

4.4.4.4 Three-step technique

There are several ways of implementing a three-step technique, the most common use phase steps of 60°, 90°, or 120°.

$\Delta\varphi_r$ = 60° = π/3 (23)

$$\Phi(x,y) = \arctan\left[\frac{2I_1 - 3I_2 + I_3}{\sqrt{3}(I_2 - I_3)}\right] \tag{24}$$

$\Delta\varphi_r$ = 90° = π/2 : φ_r = π/4, 3π/4 and 5π/4 (25)

$$\Phi(x,y) = \arctan\left(\frac{I_3 - I_2}{I_1 - I_2}\right) \tag{26}$$

$$V = \frac{\sqrt{(I_1 - I_2)^2 + (I_2 - I_3)^2}}{2I_0} \tag{27}$$

V is reduced to 0,9 V_{step} if the phase is integrated over $\Delta = \pi/2$.

$\Delta\varphi_r$ = 120° = 2π/3 ; φ_r = 0, 2π/3 and 4π/3 (28)

$$\Phi(x,y) = \arctan\left(\sqrt{3}\,\frac{I_3 - I_2}{2I_1 - I_2 - I_3}\right) \tag{29}$$

© ISO 2005 – All rights reserved
Copyright International Organization for Standardization
Reproduced by IHS under license with ISO
No reproduction or networking permitted without license from IHS
Not for Resale

$$V = \frac{\sqrt{3(I_1 - I_2)^2 + (2I_1 - I_2 - I_3)^2}}{2I_0} \tag{30}$$

V reduces to 0,83 V_{step} in case of integration over $\Delta = 2\pi/3$

For a phase shift other than $\pi/2$ or $2\pi/3$, the phase can be calculated using

$$\Phi(x,y) = \arctan\left(\frac{1-\cos\varphi}{\sin\varphi}\frac{I_1 - I_3}{2I_2 - I_1 - I_3}\right) \tag{31}$$

where phase shifts $-\varphi$, 0 and φ are assumed.

4.4.4.5 Carré technique

In the previous technique, the phase shift is known (for instance by calibration of the phase shifter, see later). With four steps, it is also possible to determine the unknown but constant phase shift φ_r.

$$\tan\left(\frac{\varphi_r}{2}\right) = \sqrt{\frac{3(I_2 - I_3) - (I_1 - I_4)}{(I_2 - I_3) + (I_1 - I_4)}} \tag{32}$$

The phase Φ at each point is

$$\Phi(x,y) = \arctan\left\{\tan\left(\frac{\varphi_r}{2}\right) \times \frac{(I_2 - I_3) + (I_1 - I_4)}{(I_2 + I_3) - (I_1 + I_4)}\right\}$$

$$= \arctan\left\{\frac{\sqrt{\left[3(I_2 - I_3) - (I_1 - I_4)\right]\left[(I_2 - I_3) + (I_1 - I_4)\right]}}{(I_2 + I_3) - (I_1 + I_4)}\right\} \tag{33}$$

For this technique the intensity modulation is

$$V = \frac{1}{2I_0}\sqrt{\frac{\left[(I_2 - I_3) + (I_1 - I_4)\right]^2 + \left[(I_2 + I_3) - (I_1 + I_4)\right]^2}{2}} \tag{34}$$

Here φ is assumed to be near $\pi/2$. If the phase shift is off by $\pm$ 10 % the estimation of V will be off by $\pm$ 10 %.

The technique works with a phase shift which does not have to be calibrated. The phase $\Phi(x,y)$ at each point in the interferogram can be determined modulo 2π, even in the case of varying phase calibration differences across the beam.

4.4.4.6 Calibrating the phase shifter

The accuracy of the above methods depends on the linearity of the phase shifter. For the typical phase shift from the piezoelectric transducer (PZT), the linearity depends on the actual driving voltage due to hysteresis and other nonlinear response effects. Therefore, a calibration of the phase-shifting equipment is necessary.

One possibility is given by the Carré technique already mentioned. A set of four intensity values is used to calculate $\Delta\varphi$. The phase shift controller should be adjusted so that the average phase shift is at the desired value and the spread in calculated phase shifts is small.

--`,,`,,,`-`-`,,`,,`,`,,`---

© ISO 2005 – All rights reserved

Copyright International Organization for Standardization
Reproduced by IHS under license with ISO
No reproduction or networking permitted without license from IHS
Not for Resale

A simpler equation can be used when taking five intensity measurements with a constant phase shift between them[8]:

$$\varphi(x,y) = \arccos\left[\frac{1}{2}\left(\frac{I_5 - I_1}{I_4 - I_2}\right)\right] \tag{35}$$

With some prior knowledge of φ, the sign ambiguities of the cosine function can be resolved.

With a separate small interferometer fed by light split off from the reference arm, and with a separate detector, the phase can also directly be measured.

With the measured values, corrected values for the phase shifter controller can be obtained (for instance a lookup table for the input voltages of the piezo driving high voltage amplifier, if a computer controls the phase shifter).

4.5 Phase measurements with spatial carrier

4.5.1 Fringe analysis by Fourier transform operations

If the spatial frequency ν_0 of the interference pattern obeys the condition $\nu_0 > \max|\mathbf{grad}\,\Phi|$, no closed fringes are present in the interferogram and one-dimensional Fourier transforms can be used to obtain the phase Φ[9].

The interference Equation (8) can be rewritten as follows:

$$I(x,y) = a(x,y) + c(x,y)\mathrm{e}^{j2\pi\nu_0 x} + c^*(x,y)\mathrm{e}^{-j2\pi\nu_0 x} \tag{36}$$

where $c(x,y) = \frac{1}{2} I_0 V \mathrm{e}^{j\Phi(x,y)}$

After a one dimensional Fourier transform the following holds:

$$F(I) = A(\nu,y) + C(\nu - \nu_0, y) + C^*(\nu + \nu_0, y) \tag{37}$$

where A, C and C^* are complex Fourier amplitudes.

By means of digital filtering, one side-band of the intensity distribution is filtered out and undergoes an inverse fast Fourier transformation (FFT). In this way the quantity $c(x,y)$ is obtained, from which the phase can be calculated:

$$\Phi(x,y) = \arctan\frac{\mathrm{Im}\,c}{\mathrm{Re}\,c} \qquad \mathrm{mod}\,\pi \tag{38}$$

or by using the complex logarithm: $\log\left[c(x,y)\right] = \log\left[\frac{1}{2}\left(I_0 V\right)\right] + j\,\Phi(x,y)$

If the sampling theorem is fulfilled (more than two detector elements per period of the cosine function), phase ambiguities can also be eliminated (see 4.4.4).

A two-dimensional approach of the FFT technique[10] can also deal with interference patterns, where the fringe density is smaller than the maximum slope of the wavefront: $\nu_0 < \max|\mathbf{grad}\,\Phi|$. For example, closed fringes are an obvious violation of this condition.

In the two-dimensional algorithm, the equation for $F(I)$ becomes

$$F(I) = A(\nu,\mu) + C(\nu,\mu) + C^*(\nu,\mu) \tag{39}$$

© ISO 2005 – All rights reserved
Copyright International Organization for Standardization
Reproduced by IHS under license with ISO
No reproduction or networking permitted without license from IHS
Not for Resale

The filtering of the complex quantity C can now be done in two orthogonal directions (with different filters in the ν and μ directions). Ambiguities can be resolved when making two separated calculations of Φ with band-pass filters oriented in orthogonal directions.

Another procedure is based on the evaluation of two interference patterns where the second pattern is shifted by about $\alpha = \pi/2$ compared to first pattern. The respective Fourier coefficients $c_1(x,y)$ and $c_2(x,y)$ can be used to calculate

$$\alpha(x,y) = \arctan\frac{\mathrm{Re}\,c_1 \cdot \mathrm{Im}\,c_2 - \mathrm{Im}\,c_1 \cdot \mathrm{Re}\,c_2}{\mathrm{Re}\,c_1 \cdot \mathrm{Re}\,c_2 + \mathrm{Im}\,c_1 \cdot \mathrm{Im}\,c_2} \tag{40}$$

α is expected to be nearly constant apart from the sign indication, which can be used to determine the sign of $\Phi(x,y)$ unambiguously.

4.5.2 Spatially synchronous fringe analysis

At the locations in the interference pattern where closed fringes appear, the local slope of the wavefront is steeper than the mean relative tilt between test and reference wavefront. At such locations, the Fourier coefficients $C(\nu,\mu)$ and $C^*(\nu,\mu)$ of the equation for $F(I)$ partially overlap and the sign is undetermined (change of sign of the calculated phase). To remove this difficulty, the relative tilt of the reference wavefront may be increased, which corresponds to a higher spatial frequency ν_0.

The underlying information about the local phase $\Phi(x,y)$ of the wavefront under test can also be extracted by multiplying the interference pattern of Equation (8) directly with cosine and sine functions that have a linear phase dependence with the same mean spatial carrier frequency as the interference pattern[11],[12]. Since the interference pattern is usually scanned, a one-dimensional representation can be used. Let f_0 be a rough estimate of the mean spatial frequency $\bar{f}$ of the interference pattern. Then

$$I(x,y)\cdot\cos(2\pi f_0 x) = a(x,y)\cos(2\pi f_0 x) + \frac{b}{2}\cos\left[\Phi(x,y) + 2\pi f_0 x\right] + \frac{b}{2}\cos\left[\Phi(x,y) - 2\pi f_0 x\right] \tag{41}$$

and

$$I(x,y)\cdot\sin(2\pi f_0 x) = a(x,y)\sin(2\pi f_0 x) + \frac{b}{2}\sin\left[\Phi(x,y) + 2\pi f_0 x\right] - \frac{b}{2}\sin\left[\Phi(x,y) - 2\pi f_0 x\right] \tag{42}$$

If the difference between the test wavefront represented by $\Phi(x,y)$ and the "reference wavefront" $2\pi f_0 x$ is small, the third term of these expressions represents a low spatial frequency component which can be extracted by a low-pass filter with a window function $H(x,y)$ (preferably of the Hanning type).

The resulting low spatial frequency Moiré can be written:

$$M_1 = \frac{1}{2} I_0 V \cos\left[\Phi(x,y) - 2\pi(\bar{f} - f_0)x\right] \tag{43}$$

$$M_2 = \frac{1}{2} I_0 V \sin\left[\Phi(x,y) - 2\pi(\bar{f} - f_0)x\right] \tag{44}$$

and

$$\Phi(x,y) - 2\pi f_0 x = \arctan\frac{M_2(x,y)}{M_1(x,y)} \tag{45}$$

Since the convolution window shall be several fringes wide, a high fringe density is needed in order for each phase measurement to be located to a region much smaller than the overall size of the pupil. This also keeps the loss of phase information small where the convolution window overlaps the edge of the pupil.

© ISO 2005 – All rights reserved

Copyright International Organization for Standardization
Reproduced by IHS under license with ISO
No reproduction or networking permitted without license from IHS
Not for Resale

The simplest implementation of the quadrate multiplicative Moiré (QMM) involves a pure one-dimensional reference containing pure tilt, and is applicable to interferograms to which a large tilt component has been added, eliminating closed fringes. In this case, M_1 and M_2 reduce to:

$$\overline{M_1} = \sum_{i=-N}^{N} I(x_i, y)\cos(2\pi f_0 x_i)\, H(x - x_i, y) \tag{46}$$

$$\overline{M_2} = \sum_{i=-N}^{N} I(x_i, y)\sin(2\pi f_0 x_i)\, H(x - x_i, y) \tag{47}$$

and $\Phi(x, y) = \arctan\dfrac{\overline{M_2}}{\overline{M_1}}$

In another version, the high frequency component of the equation is extracted by filtering with a filter frequency f_0. Then:

$$F_1(x, y) = \sum_{i=-N}^{N} I(x_i, y)\cos\left[2\pi f_0 (x - x_i)\right]\, H(x - x_i, y) \tag{48}$$

and

$$F_2(x, y) = \sum_{i=-N}^{N} I(x_i, y)\sin\left[2\pi f_0 (x - x_i)\right] H(x - x_i, y) \tag{49}$$

is calculated, resulting in the phase

$$\Phi(x, y) = \arctan\frac{F_2(x, y)}{F_1(x, y)} \tag{50}$$

This method is called “sinusoidal window algorithm”.

A third method makes use of a complex exponential window to filter out the phase information of a single side lobe of the Fourier transform

$$h' = h(x, y)\mathrm{e}^{j2\pi f_0 x} \tag{51}$$

resulting in a function which real and imaginary parts are identical to F_1 and F_2 of the sinusoidal window method. The phase is then given by the arctangent of the ratio of real and imaginary parts.

4.6 Removal of phase ambiguities (phase unwrapping)

The above equations allow the determination of the phase modulo π. In order to determine the phase difference between the interfering wavefronts without ambiguity, the following additional steps shall be performed[6].

a) In a first step, the determination of phase modulo 2π requires to take the signs of the numerator ($\sin\Phi$) and the denominator ($\cos\Phi$) in the arctangent expression of the phase into account. The phase is calculated modulo $\pi/2$ using absolute values in the nominator and denominator, then the signs of these quantities are used according to Table 5 to calculate the phase modulo 2π.

© ISO 2005 – All rights reserved
Copyright International Organization for Standardization
Reproduced by IHS under license with ISO
No reproduction or networking permitted without license from IHS
Not for Resale

For the Carré technique, two other quantities instead of ($\sin\Phi$) and ($\cos\Phi$) have to be examined in the same way:

$$(I_1 - I_3) = \left[2I_0 V \sin\varphi\right]\sin\Phi \tag{52}$$

and

$$(I_2 + I_3) - (I_1 + I_4) = \left[2I_0 V \cos\varphi \sin^2\varphi\right]\cos\Phi \tag{53}$$

b) Provided that the sampling requirement is fulfilled and the phase difference between adjacent pixels exceeds π a phase jump will occur and a phase of 2π should be added with the sign of the phase of the previous pixel. This procedure should be carried out in two dimensions, first for one diameter and then in the perpendicular direction from this diameter proceeding over the rest of the aperture.

In this way, a continuous phase function can be obtained from the raw phase data.

Table 6 — Determination of the phase modulo 2π

Numerator ($\sin\Phi$)	Denominator ($\cos\Phi$)	Adjusted phase	Range of phase values
positive	positive	Φ	$0 - \frac{\pi}{2}$
positive	negative	$\pi - \Phi$	$\frac{\pi}{2} - \pi$
negative	negative	$\pi + \Phi$	$\pi - \frac{3\pi}{2}$
negative	positive	$2\pi - \Phi$	$\frac{3\pi}{2} - 2\pi$
0	anything	π	π
negative	0	$\frac{\pi}{2}$	$\frac{\pi}{2}$
positive	0	$\frac{3}{2}\pi$	$\frac{3}{2}\pi$

4.7 Registration of wavefronts; coordinate systems, coordinate system definition

In direct phase measuring interferometers, wavefront phase or surface figure data are recorded on a CCD camera. At each x_p, y_p pixel location on the camera where there is *phase modulated intensity data*, a phase or height value is recorded. Some measured objects will fill the entire CCD array, while others will fill only part of it. When the entire array contains data, the centre of the array is the centre or origin of the processed data set. The ratio of the number of pixels vertically to horizontally needed to describe a circle is the *aspect ratio*.

When only part of the array is filled with phase data, the origin of the *processed data* is the centre of gravity (or centroid) of the data set. For data from a circular object, the coordinate system of the object being measured will be shown how it is related to the *pixel coordinates*. For most CCD cameras, the pixels are not square but rectangular. However, it is desirable that a circular object be displayed and analyzed as circular. Both the centring and the aspect ratio of the pixels are accounted for by the following method. Using all the modulated phase data, the mean x_p and y_p are found by summing the x and y locations of every modulated data pixel. This mean, x_0, y_0, of the x_p and y_p, gives the centre of the data set in pixel coordinates. The coordinates (x_{pc}, y_{pc}) of the *centred pixel data* set is then

$$x_{pc} = x_p - x_0 \text{ and } y_{pc} = y_p - y_0 \tag{54}$$

The centred pixel data set are then used to determine the statistics of the data by using various processing algorithms described below.

© ISO 2005 – All rights reserved

Copyright International Organization for Standardization
Reproduced by IHS under license with ISO
No reproduction or networking permitted without license from IHS
Not for Resale

Another issue regarding coordinate systems is the mapping of a curved surface onto the plane CCD detector. For a plane surface the lateral (x,y) coordinates of the object are mapped linearly onto the CCD detector. For a powered surface, however, particularly a surface with a high numerical aperture, there is a question of how the surface is mapped onto the detector. For most interferometers, the object under test is mapped onto that object's pupil plane, a plane at the object's vertex. The mapping is given by rays that appear to come from infinity so they are parallel to the optical axis. Thus the x,y coordinates of the surface under test are mapped one-to-one to the pupil plane while the component of sag in the direction of the optical axis is suppressed. The pupil plane is mapped linearly onto the detector just as in the case of a plane surface.

There are two consequences that follow immediately from this.

— A plane grid of straight lines perpendicular to the optical axis placed between the object and the interferometer will be imaged on the detector with pincushion distortion.

— Also, the x,y coordinates in the pupil plane are the same x,y coordinates that appear in all the analysis of the phase data, that is, all the analysis gives height or topographic departures from a plane surface.

4.8 Polynomial and other representations of wavefronts

4.8.1 Representation of phase data

Once the phase data is transformed or mapped from detector or pixel coordinates into *analysis coordinates*, it can be represented in basically two different ways. It can be left as discrete data points or it can be interpolated with an analytic function into a global representation expressed by a number of coefficients. Each method has advantages and disadvantages depending on how the data are to be used. Neither method is optimum in all cases. In some methods of analysis, it is best to represent the low *spatial frequency* part of the data by analytic functions and the high spatial frequency part by the raw pixelated data.

Leaving the phase data as discrete data points, or pixelated data, has the advantage that it is essentially *raw data*. It has the maximum intrinsic information about the object under test. As with any sampled data set, there is no, or too little information about the object on a spatial scale of less than 2 pixels, the Nyquist limit. But there is detailed information about the surface up to the Nyquist limit.

The disadvantage of leaving the data pixelated is that many useful aspects of the data are not obvious from this large number of essentially unrelated data points. Also to derive most statistical parameters from the data, the entire data set shall by processed to determine each different parameter.

If the pixelated data is fit to 2-D analytic functions, many properties of the data set are obvious from inspection or can be calculated simply from the coefficients representing the function. The entire data set is no longer needed to get most of the surface information out of it. Also, if certain analytic functions are used, many properties of how well an imaging system will work can be determined directly from the functional coefficients.

The disadvantage of fitting to the raw data is that the fitting process is a filter and some of the information is lost, particularly the high spatial frequency part. If the raw data are ever deleted from memory there is no way of recovering them from the analytic function.

Analytic functions for describing surfaces with either circular or rectangular boundaries are defined in 4.8.2 to 4.8.6. For details see Annex A.

4.8.2 Zernike polynomials for a circular boundary

Because most optical systems have circular pupils, a particularly useful set of analytic functions for representing optical surface and wavefront data are the Zernike polynomials. This particular set of polynomials is complete and orthogonal over the unit circle. In addition, with appropriate normalization, the coefficients of the Zernike polynomials are the r.m.s. values of the individual optical aberrations present in the phase data and these directly relate to the imaging properties of optical systems.

© ISO 2005 – All rights reserved
Copyright International Organization for Standardization
Reproduced by IHS under license with ISO
No reproduction or networking permitted without license from IHS
Not for Resale

It should be pointed out immediately that the useful properties of Zernike polynomials apply only to circular apertures (or their close relatives, see 5.7.3 and 5.7.4) and that very misleading results will be obtained by applying Zernike fitting to non-circular data sets. For square or rectangular data sets, see 5.7.5. For situations where the clear aperture is elliptical, it is usually this way because a circular beam is incident on a mirror at a 45° (or some other large) angle of incidence. In this case, the correct amount of astigmatism over the elliptical aperture is the equivalent of power at normal incidence. For this reason, in 5.7.3, it is suggested to rescale the aperture coordinates to make the pupil circular, to evaluate the error with the regular Zernike polynomials and then to scale the aperture back to its elliptical shape. Annex A shows the first six orders of Zernike polynomials normalized in two ways depending on their application. The notation used is that of Reference [13] with subscripts and superscripts. This differs from the recent historical practice of several different "serial numbering" schemes used for ease of computer coding. One advantage of the Zernike polynomials is their characterization of the symmetry properties of the aberrations. These symmetries are immediately obvious if the indices of the polynomials and their coefficients are given as subscripts and superscripts, the subscript giving the radial order and the superscript giving the angular or azimuthal order. The symmetry properties of the first few orders are obvious. A further advantage is that the Zernike order is obvious from inspection rather than being familiar with a proprietary scheme.

Two methods of normalization are given in Annex A, the extreme value or peak-to-valley method designated with an upper case letter and the r.m.s. method designated by a lower case letter. Again, for recent historical reasons, the first widely accepted publication of the Zernike polynomials for the reduction of interferometric data used the peak-to-valley method where a coefficient with a value of 1 meant a peak-to-valley error of that term of 2 units. This usage was also compatible with the shop floor method of interpreting test plate interferometric patterns. However, the r.m.s. method is more useful when wanting to determine the effect of one or more aberrations on the imaging performance of an optical system and eliminates the need for an understanding of exactly what peak-to-valley means.

For the purposes of this part of ISO 14999, the following convention regarding normalization is adopted. If the Zernike coefficients are designated with an upper case or capital letter such as A_2^0, it will mean that peak-to-valley normalization is being used. If the coefficients are written as lower case letters such as a_2^0, it means the r.m.s. normalization is being used. Conversion from one normalization to the other is achieved by multiplying peak-to-valley coefficients by the normalization factor shown in Annex A to get the r.m.s. coefficients.

A useful initial operation to perform with the Zernike representation is to remove the piston, tip and tilt present in almost every set of interferometric data. Notice the r.m.s. error is just the root sum square of the coefficients.

Similarly, higher order coefficients can be set to zero to see the effect of removing higher order aberrations. The r.m.s. error of the remaining surface or wavefront error is still the root sum square of the coefficients.

For pixel-based data, the r.m.s. error in a surface or wavefront is just $(1/N)\ [\sum(z^2)]^{1/2}$ where N is the number of data pixels within the clear aperture and z is the height above or below the mean reference plane. The sum is over all N data points.

For data fitted to Zernike polynomials using the r.m.s. normalization, the r.m.s. error in a surface or wavefront is $[\sum(a_j^k)^2]^{1/2}$, where the sum is over all the Zernike coefficients remaining after coefficients have been set to zero to remove tilt, focus, etc.

4.8.3 Use of Zernike polynomials for an elliptical boundary

Elliptical apertures generally occur in optical systems because a collimated beam of light is reflected from a plane mirror to fold the beam path. As in many optical systems, a small amount of power in the optical path is of little consequence because it can usually be focused out in the image plane. However, if a plane mirror has a little power and is used in non-normal incidence the mirror will introduce astigmatism, which will degrade the optical performance of the system.

On the other hand, if the plane mirror has astigmatism aligned with the plane of incidence then this astigmatism will appear as power in the system and may be focused out. Thus, the main use for Zernike polynomials in the analysis of elliptical apertures is to determine the magnitude and orientation of power and astigmatism in the mirror surface.

© ISO 2005 – All rights reserved

Copyright International Organization for Standardization
Reproduced by IHS under license with ISO
No reproduction or networking permitted without license from IHS
Not for Resale

The following procedure will permit the analysis of phase data over an elliptical aperture. First, assume the major axis, a, of the aperture is aligned along the x-axis. Let a and b be the lengths of the semi-major and minor axes of the ellipse. Multiply the x coordinates of all the data locations by the ratio (b/a). The pupil will now be circular. Fit Zernike polynomials as usual.

If the optical system will allow power to be focused out then the a_2^0 coefficient times 2 times the cosine of the angle of incidence at which the mirror will be used is a measure of the peak-to-valley power introduced by the mirror. Any astigmatism or other aberration terms will degrade the wavefront and should be considered as irregularity. After power (a_2^0) is removed the peak-to-valley magnitude over the remaining irregularity needs to be multiplied by the cosine of the angle of incidence in the system to determine its effect on the wavefront. The comments above assume the mirror surface is tested at normal incidence. If it is tested at the angle in which it will be used the test will give a direct measure of the irregularity.

Once Zernike polynomials have been fitted to the circle aperture data, a contour map of the surface over the elliptical aperture can be made by multiplying the x coordinates of the circular data by the ratio (a/b) and plotting the results.

There may be other occasions for fitting Zernike polynomials to data from an elliptical clear aperture. The approach suggested above may also be used in this case provided there is a clear understanding of how scaling the aperture coordinates in one direction affects the results of the fitting.

4.8.4 Zernike-Tatian polynomials for a circular shape with a central hole (annular)

In the case of an interferogram of an annular aperture, such as might be obtained when testing a Cassegrain type telescope, the annular aperture can be fitted with modified Zernike polynomials as listed Annex A. These polynomials are a function of ε, the ratio of the inner radius of the annulus to the unit outer radius of the annulus. In all other attributes, they are the same as the Zernike polynomials for the full circular aperture.

4.8.5 Legendre polynomials for a rectangle boundary

There are times when it is convenient to represent a rectangular aperture with a 2-D analytic function such as when testing cylindrical optics. When this is necessary, Legendre polynomials are an appropriate choice.

4.8.6 Orthogonal functions on “unusual areas”

It is possible to compute orthogonal polynomials, given certain desired characteristics, over an arbitrarily shaped area, including a weight function, if desired. Mathematically, this is not a new method but it does not seem to be applied in the optics world. The term orthogonal *function*, and not *polynomial*, is used in this text as this method applies to absolutely any base of functions. This could include, e.g. $R(1-\cos\Theta)$, to accurately model defocus.

Shown in Annex B are a few examples of orthogonal polynomials, without showing the details of the computation. This computation can be very simple using matrix notation, enabling the generation of the polynomials one after the other, in a deterministic way (no iterations or approximations).

5 Test reports and calibration certificates

5.1 General

The results of each test, calibration, or series of tests or calibrations carried out by a laboratory should be reported accurately, clearly and objectively, and in accordance with any specific instructions in the test or calibration procedures.

The results should be reported, usually in a test report or a calibration certificate, and should include all the information requested by the client and necessary for the interpretation of the test or calibration results. This information is normally that required by 5.2, and 5.3 or 5.4

© ISO 2005 – All rights reserved
Copyright International Organization for Standardization
Reproduced by IHS under license with ISO
No reproduction or networking permitted without license from IHS
Not for Resale

5.2 Content of test reports and calibration certificates

Each test report or calibration certificate should include at least the following information, unless the laboratory has valid reasons for not doing so:

a) a title (e.g. “Test report” or “Calibration certificate”);

b) the name and address of the laboratory, and the location where the test or calibration was carried out if different from the address of the laboratory;

c) unique identification of the test report or calibration certificate, such as a serial number, on each page;

d) the name and address of the client;

e) a brief description of the method of measurement used;

f) a brief description, including unambiguous identification, of the item(s) tested or calibrated;

g) the date(s) of performance of the test or calibration;

h) the test or calibration results with the units of measurement;

i) the name, function and signature of the person authorizing the test report or calibration certificate.

Hard copies of test reports and calibration certificates should also include the page number and the total number of pages, e.g. Page 1 of 3.

It is recommended that laboratories should also include a statement specifying that the test report or calibration certificate shall not be reproduced except in full.

5.3 Test reports

In addition to the requirements listed in 5.2, test reports should, where necessary for the interpretation of the test results, include the following:

a) deviations from, additions to, or exclusions from the test method and information on specific test conditions, such as environmental conditions;

b) where relevant, a statement of compliance/non-compliance of the test item(s) with requirements or specifications;

c) where applicable, a statement on the estimated uncertainty of measurement (information on uncertainty of measurement is needed in test reports when it is relevant to the validity or application of the test results, when a client’s instructions so require, or when the uncertainty affects compliance to a specification limit);

d) where appropriate and needed, opinions and interpretations based on the measurement results;

e) additional information which may be required by specific methods or clients.

5.4 Calibration certificates

5.4.1 Basics

In addition to the requirements listed in 5.2, calibration certificates should include the following, where necessary for the interpretation of calibration results:

a) the conditions (e.g. environmental) under which the calibrations were made that have an influence on the measurement results;

© ISO 2005 – All rights reserved

Copyright International Organization for Standardization
Reproduced by IHS under license with ISO
No reproduction or networking permitted without license from IHS
Not for Resale

b) the uncertainty of measurement and/or a statement of compliance with an identified metrological specification or clauses thereof;

c) evidence that the measurements are traceable to national standards.

5.4.2 Specification

The calibration certificate should relate only to quantities and the results of functional tests. If a statement relating to compliance with a specification is made, this should identify which clauses of the specification are met or not met.

When a statement of compliance with a specification is made omitting the measurement results and associated uncertainties, the laboratory should record those results and retain them for possible future reference.

When statements of compliance are made, the uncertainty of measurement shall be taken into account.

5.4.3 Adjustment or repair

When an instrument/device for calibration has been adjusted or repaired, the calibration results before and after adjustment or repair, if available, should be reported.

5.5 Opinions and interpretations

When opinions and interpretations are included, the laboratory should document the basis upon which the opinions and interpretations have been made. Opinions and interpretations should be clearly marked as such in a test report.

Opinions and interpretations included in a test report may comprise, but not be limited to, the following:

— an opinion on the statement of compliance/non-compliance of the results with requirements;

— recommendations on how to use the results;

— guidance to be used for improvements.

In cases where it is appropriate to communicate opinions and interpretations by direct dialogue with the client, that dialogue should also be written down.

5.6 Electronic transmission of results

In the case of transmission of test or calibration results by telephone, telex, facsimile or other electronic means, the requirements of this part of ISO 14999 should be met.

5.7 Format of reports and certificates

The format should be designed to accommodate each type of test or calibration carried out and to minimize the possibility of misunderstanding or misuse.

Attention should be given to the layout of the test report and calibration certificate, especially with regard to the presentation of the test and calibration data and ease of assimilation by the reader.

The headings used within the report or certificate should be standardized as far as possible.

--`,,```,,,--`,,`,,`,`,,`---
© ISO 2005 – All rights reserved
Copyright International Organization for Standardization
Reproduced by IHS under license with ISO
No reproduction or networking permitted without license from IHS
Not for Resale

5.8 Amendments to test reports and calibration certificates

Material amendments to a test report or calibration certificate after issue should be made only in the form of a further document, or data transfer, which includes a statement indicating that it is a “Supplement to test report, serial number (XXXX)” or the equivalent for a calibration certificate.

When it is necessary to issue a completely new test report or calibration certificate, this should be uniquely identified and should contain a reference to the original that it replaces.

6 Data format

Information concerning data formats used in interferometric computational processes can be found for example at http://support.zygo.com/resource/manuals.cgi?type=mp or at http://www.fisba.ch/ (Metrology-Products-Software).

© ISO 2005 – All rights reserved

Copyright International Organization for Standardization
Reproduced by IHS under license with ISO
No reproduction or networking permitted without license from IHS
Not for Resale

Annex A
(informative)

Orthogonal polynomials

A.1 General

Various polynomial sets are described here, to be used on the two most widely used area shapes in optics:

a) Circular area (extendible to the elliptical area);

b) Square area (extendible to the rectangular area).

Each set is designated by a combination of letters:

— Area shape: C (circle/ellipse); S (square/rectangle);

— Generation basis: P (polar); R (rectangular);

— Form of expression: Z (Zernike), P (polar); R (rectangular).

NOTE 1 In this Annex, the terms “polynomial” and “function” are sometimes used interchangeably. For example, a Zernike *function* may be obtained by multiplying a Zernike *polynomial* by a *harmonic* function [namely, $\cos(\phi)$, $\sin(\phi)$]. However, expressed in Cartesian coordinates, Zernike functions become *polynomials* with respect to (x, y).

NOTE 2 The orthogonal sets described here are orthogonal on continuous areas of the appropriate shape (circle or square). Using these sets for discrete, which is always the case with real data, results in non-orthogonality of the said functions. It is up to the user to determine the degree to which this non-orthogonality perturbs the coefficient computation. However, it can be said that for metrology devices common today, the discrepancy is negligible for the lower order functions.

CAUTION — Any orthogonal set is to be used with caution. When applied to *real* data (as opposed to, e.g. studying the *mathematics* of aberrations), the individual orthogonal functions are unrelated to the data to be analysed.

The reason why the orthogonal sets described here are useful for *practical* analysis is the form of first few terms, namely “piston”, “tip”, “tilt”, “power”, which describe changes in conjugates, and also some useful lower order aberrations: “coma”, “astigmatism”, “spherical aberration”.

The universally used Zernike set (A.3.1), as well as the alternative set (A.3.3), include these useful terms. The Legendre set (A.3.2) does not include all these terms (in particular, it has no “power” term).

However, above these lower orders, the terms of any orthogonal set become quite meaningless in *practice*. Optical components rarely exhibited, for example are a pure Z20, L17 or B29 shape.

© ISO 2005 – All rights reserved
Copyright International Organization for Standardization
Reproduced by IHS under license with ISO
No reproduction or networking permitted without license from IHS
Not for Resale

Table A.1 — Orthogonal set summary

No.	Reference	Name	Area	Symmetry	Coordinates	Form (see notes)	Note
Table A.2	C-P-P	Circular / Zernike	Circle (ellipse)	Polar	Polar	$\{P_n(r)\cos(m\theta)\}$ $\{Q_n(r)\sin(m\theta)\}$	Zernike { Z }
Table A.3	S-R-R	Square / Legendre	Square (rectangle)	Rectangular	Rectangular	$L_p(x)\,L_q(x) = \Sigma\{c_{p,q}\,(x_p\,y_q)\}$	Legendre { L }
Table A.4	S-P-Z	Square / Polar	Square (rectangle)	Polar	Polar	Combination of Zernike functions	New set { B }
Table A.5	S-P-P	Square / Polar	Square (rectangle)	Polar	Polar	$\{P_n(r)\cos(m\theta)\}$ $\{Q_n(r)\sin(m\theta)\}$	New set { B }
NOTE 1	$P_n(r)$, $Q_n(r)$ denote polynomials for the variable "r".						
NOTE 2	n, m, p, q are non-negative integers.						
NOTE 3	More information may be obtained, e.g. on http://www.mboptique.com.						

A.2 Coefficient computation

When fitting a given set of orthogonal functions $\{P_0, P_1, P_2 \ldots\}$ to a function "f", coefficients $\{a_0, a_1, a_2 \ldots\}$ of the orthogonal functions are computed as follows:

$$a_i = \frac{\iint_A P_i(u,v)\,f(u,v)\,\mathrm{d}A}{\iint_A P_i(u,v)\,P_i(u,v)\,\mathrm{d}A} = \frac{1}{s^2_{\mathrm{rms},i}}\iint_A P_i(u,v)\,f(u,v)\,\mathrm{d}A$$

where

(u,v) are the space coordinates;

A is the area of integration and $\mathrm{d}A$ is the area increment;

$s^2_{\mathrm{rms},i}$ is the r.m.s.-squared value of orthogonal polynomial (P_i).

s^2_{rms} values are tabulated below. However, because the orthogonality of the sets over discrete areas is not strict, it is advised to perform the actual computation of the s^2_{rms} values when they are required, rather than using the values tabulated here.

A.3 Definitions, tables and illustration of orthogonal functions

NOTE $C^i_n = \mathrm{Comb}(n,i) = \frac{n\ !}{i\ !\ (n-i)\ !}$

A.3.1 Circular areas: Zernike functions ("C-P")

A.3.1.1 General

This is the classical Zernike set, which is widely used in optics. It is orthogonal over the circular area (extendible to the elliptical area).

Its definitions are given in A.3.1.2. s^2_{rms} values are given in Table A.2 and an illustration of the orthogonal set (Z 0 – Z 35) is given in Figure A.1.

© ISO 2005 – All rights reserved

Copyright International Organization for Standardization
Reproduced by IHS under license with ISO
No reproduction or networking permitted without license from IHS
Not for Resale

A.3.1.2 Definitions

Indices: $(n + m) = N$: Order of the function;
$(n - m) \geqslant 0$: m is not greater than n;
$(n - m)$ is even.

Area of definition: Circle, radius equal to 1.

Zernike polynomial: $$Z(n,m,r) = \sum_{i=0}^{n-m} -1^{i} \left[\frac{(n-i)\ !}{i\ !\ \left(\frac{n+m}{2}-i\right)\ !\ \left(\frac{n-m}{2}-i\right)\ !} \right] r^{n-2i}$$

Principal term: $$\left[\frac{n!}{\left(\frac{n+m}{2}\right)\ !\ \left(\frac{n-m}{2}\right)\ !} \right] r^{n} = C_{n}^{\left(\frac{n+m}{2}\right)} r^{n} = C_{n}^{(N/2)} r^{n}$$

Polynomial mean-square value (s_{rms}^{2}) : $\left\| Z(n,\ m,\ r) \right\|^{2} = 1/(n+1)$

Zernike function (orthogonal series for use in optics) : $Z(n,m,r,\theta) = Z(n,m,r) \times \begin{vmatrix} \cos(m\theta) \\ \sin(m\theta) \end{vmatrix}$

NOTE The mean-square value of the Zernike *functions* is modified by the cosine or sine functions. For these functions ($m > 0$), the mean-square value is half that of the corresponding Zernike *Polynomial*. For the rotationally-symmetrical functions ($m = 0$), the mean-square values are equal to those of the corresponding polynomial.

© ISO 2005 – All rights reserved
Copyright International Organization for Standardization
Reproduced by IHS under license with ISO
No reproduction or networking permitted without license from IHS
Not for Resale

Table A.2 — Circular — Zernike ("C-P-P")

Orthogonal on the circle (extendible to the ellipse) **Polar variables:** (r, θ) **Expressed in polar coordinates:** $\Sigma\{P_n(r)\cos(m\theta)\}$ **or** $\Sigma\{P_n(r)\sin(m\theta)\}$; $N = n + m$				
Z	N	n, m	**Formula**	s^2_{rms}
Z0	0	0, 0	1	1
Z1	2	1, 1	$r\cos\theta$	1 / 4
Z2	:	1, 1	$r\sin\theta$	1 / 4
Z3	2	2, 0	$2r^2 - 1$	1 / 3
Z4	4	2, 2	$r^2\cos2\theta$	1 / 6
Z5	:	2, 2	$r^2\sin2\theta$	1 / 6
Z6	:	3, 1	$(3r^2 - 2)\, r\cos\theta$	1 / 8
Z7	:	3, 1	$(3r^2 - 2)\, r\sin\theta$	1 / 8
Z8	4	4, 0	$6r^4 - 6r^2 + 1$	1 / 5
Z9	6	3, 3	$r^3\cos3\theta$	1 / 8
Z10	:	3, 3	$r^3\sin3\theta$	1 / 8
Z11	:	4, 2	$(4r^2 - 3)\, r^2\cos2\theta$	1 / 10
Z12	:	4, 2	$(4r^2 - 3)\, r^2\sin2\theta$	1 / 10
Z13	:	5, 1	$(10r^4 - 12r^2 + 3)\, r\cos\theta$	1 / 12
Z14	:	5, 1	$(10r^4 - 12r^2 + 3)\, r\sin\theta$	1 / 12
Z15	6	6, 0	$20r^6 - 30r^4 + 12r^2 - 1$	1 / 7
Z16	8	4, 4	$r^4\cos4\theta$	1 / 10
Z17	:	4, 4	$r^4\sin4\theta$	1 / 10
Z18	:	5, 3	$(5r^2 - 4)\, r^3\cos3\theta$	1 / 12
Z19	:	5, 3	$(5r^2 - 4)\, r^3\sin3\theta$	1 / 12
Z20	:	6, 2	$(15r^4 - 20r^2 + 6)\, r^2\cos2\theta$	1 / 14
Z21	:	6, 2	$(15r^4 - 20r^2 + 6)\, r^2\sin2\theta$	1 / 14
Z22	:	7, 1	$(35r^6 - 60r^4 + 30r^2 - 4)\, r\cos\theta$	1 / 16
Z23	:	7, 1	$(35r^6 - 60r^4 + 30r^2 - 4)\, r\sin\theta$	1 / 16
Z24	8	8, 0	$70r^8 - 140r^6 + 90r^4 - 20r^2 + 1$	1 / 9
Z25	10	5, 5	$r^5\cos5\theta$	1 / 12
Z26	:	5, 5	$r^5\sin5\theta$	1 / 12
Z27	:	6, 4	$(6r^2 - 5)\, r^4\cos4\theta$	1 / 14
Z28	:	6, 4	$(6r^2 - 5)\, r^4\sin4\theta$	1 / 14
Z29	:	7, 3	$(21r^4 - 30r^2 + 10)\, r^3\cos3\theta$	1 / 16
Z30	:	7, 3	$(21r^4 - 30r^2 + 10)\, r^3\sin3\theta$	1 / 16
Z31	:	8, 2	$(56r^6 - 105r^4 + 60r^2 - 10)\, r^2\cos2\theta$	1 / 18
Z32	:	8, 2	$(56r^6 - 105r^4 + 60r^2 - 10)\, r^2\sin2\theta$	1 / 18
Z33		9, 1	$(126r^8 - 280r^6 + 210r^4 - 60r^2 + 5)\, r\cos\theta$	1 / 20
Z34	:	9, 1	$(126r^8 - 280r^6 + 210r^4 - 60r^2 + 5)\, r\sin\theta$	1 / 20
Z35	10	10, 0	$252r^{10} - 630r^8 + 560r^6 - 210r^4 + 30r^2 - 1$	1 / 11
Z36	12	6, 6	$r^6\cos6\theta$	1 / 14
Z37	:	6, 6	$r^6\sin6\theta$	1 / 14
Z38	:	7, 5	$(7r^2 - 6)\, r^5\cos5\theta$	1 / 16
Z39	:	7, 5	$(7r^2 - 6)\, r^5\sin5\theta$	1 / 16
Z40	:	8, 4	$(28r^4 - 42r^2 + 15)\, r^4\cos4\theta$	1 / 18
Z41	:	8, 4	$(28r^4 - 42r^2 + 15)\, r^4\sin4\theta$	1 / 18
Z42	:	9, 3	$(84r^6 - 168r^4 + 105r^2 - 20)\, r^3\cos3\theta$	1 / 20
Z43	:	9, 3	$(84r^6 - 168r^4 + 105r^2 - 20)\, r^3\sin3\theta$	1 / 20
Z44	:	10, 2	$(210r^8 - 504r^6 + 420r^4 - 140r^2 + 15)\, r^2\cos2\theta$	1 / 22
Z45	:	10, 2	$(210r^8 - 504r^6 + 420r^4 - 140r^2 + 15)\, r^2\sin2\theta$	1 / 22
Z46	:	11, 1	$(462r^{10} - 1\,260r^8 + 1\,260r^6 - 560r^4 + 105r^2 - 6)\, r\cos\theta$	1 / 24
Z47	:	11, 1	$(462r^{10} - 1\,260r^8 + 1\,260r^6 - 560r^4 + 105r^2 - 6)\, r\sin\theta$	1 / 24
Z48	12	12, 0	$924r^{12} - 2\,772r^{10} + 3\,150r^8 - 1\,680r^6 + 420r^4 - 42r^2 + 1$	1 / 13

© ISO 2005 – All rights reserved
Copyright International Organization for Standardization
Reproduced by IHS under license with ISO
No reproduction or networking permitted without license from IHS
Not for Resale

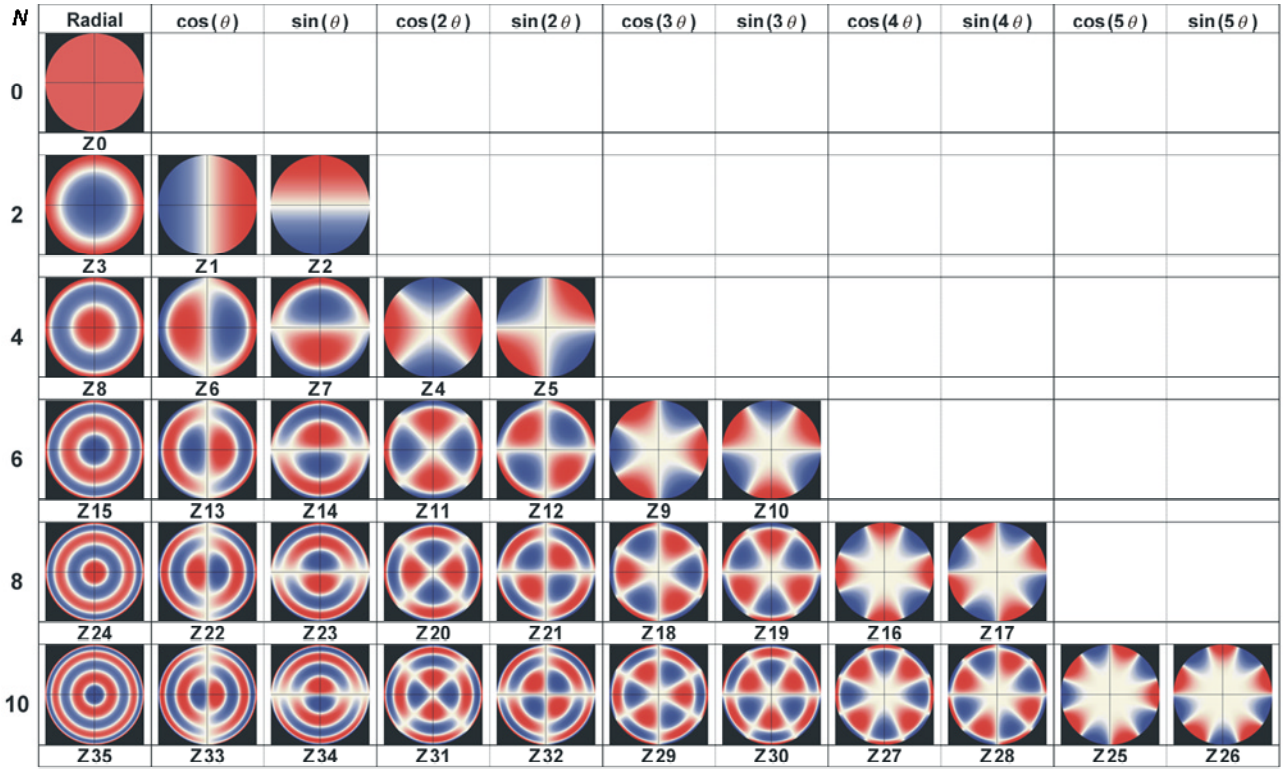

Figure A.1 — Example of visualisation of Zernike orthogonal set (Z0 – Z35)

A.3.2 Square areas — Legendre functions ("S-R")

A.3.2.1 General

Legendre polynomials are 1D polynomials. By multiplying two such polynomials, one for each direction (x and y), one obtains a 2D set of polynomials (functions) orthogonal on a square (extendible to the rectangular area).

The definitions are given in A.3.2.2. s^2_{rms} values are given in Table A.3 and an illustration of the orthogonal set (L0 – L35) is given in Figure A.2.

A.3.2.2 Definitions

Indices: $(p, q) = N$: Order of the function;
p, q : Non-negative integers.

Area of definition : Centred square, length of sides equal to 2.

Legendre polynomial (1D): $$L(p,x) = \sum_{i=0}^{p/2} -1^i C_p^i C_{2(p-i)}^p \, r^{p-2i}$$

Principal term: $$C_{2p}^p \; x^p = \frac{(2p)!}{(p!)^2} x^p$$

1D Polynomial mean-square value (s^2_{rms}): $$\left\| L(p,x) \right\|^2 = 1/(2p+1)$$

--`,,`,,,,-`-`,,`,,`,`,,`---
Copyright International Organization for Standardization
Reproduced by IHS under license with ISO
No reproduction or networking permitted without license from IHS
Not for Resale
© ISO 2005 – All rights reserved

2D Legendre polynomial (orthogonal series for use in optics): $L(p,q,x,y) = L(p,x) \times L(q,y)$

2D Polynomial mean-square value: $\left\| L(p,q,x,y) \right\|^2 = 1/\left[(2p+1)(2q+1) \right]$

--`,,`,,,,-`-`,,`,,`,`,,`---

© ISO 2005 – All rights reserved

Copyright International Organization for Standardization
Reproduced by IHS under license with ISO
No reproduction or networking permitted without license from IHS
Not for Resale

Table A.3 — Square — Legendre ("S-R-R")

Orthogonal on the square (extendible to the rectangle)

Cartesian variables: (x, y)

Expressed in rectangular coordinates: $\Sigma\, a_{p,q}\, (x^p \cdot y^q)$; $N = p + q$

L	N	p, q	Formula	s^2_{rms}
L0	0	0, 0	1	1
L1	1	1, 0	x	1 / 3
L2	1	0, 1	y	1 / 3
L3	2	2, 0	$(3x^2 - 1) / 2$	1 / 5
L4	:	1, 1	xy	1 / 9
L5	2	0, 2	$(3y^2 - 1) / 2$	1 / 5
L6	3	3, 0	$x(5x^2 - 3) / 2$	1 / 7
L7	:	2, 1	$y(3x^2 - 1) / 2$	1 / 15
L8	:	1, 2	$x(3y^2 - 1) / 2$	1 / 15
L9	3	0, 3	$y(5y^2 - 3) / 2$	1 / 7
L10	4	4, 0	$(35x^4 - 30x^2 + 3) / 8$	1 / 9
L11	:	3, 1	$xy(5x^2 - 3) / 2$	1 / 21
L12	:	2, 2	$(3y^2 - 1)(3x^2 - 1) / 4$	1 / 25
L13	:	1, 3	$xy(5y^2 - 3) / 2$	1 / 21
L14	4	0, 4	$(35y^4 - 30y^2 + 3) / 8$	1 / 9
L15	5	5, 0	$x(63x^4 - 70x^2 + 15) / 8$	1 / 11
L16	:	4, 1	$y(35x^4 - 30x^2 + 3) / 8$	1 / 27
L17	:	3, 2	$x(3y^2 - 1)(5x^2 - 3) / 4$	1 / 35
L18	:	2, 3	$y(5y^2 - 3)(3x^2 - 1) / 4$	1 / 35
L19	:	1, 4	$x(35y^4 - 30y^2 + 3) / 8$	1 / 27
L20	5	0, 5	$y(63y^4 - 70y^2 + 15) / 8$	1 / 11
L21	6	6, 0	$(231x^6 - 315x^4 + 105x^2 - 5) / 16$	1 / 13
L22	:	5, 1	$xy(63x^4 - 70x^2 + 15) / 8$	1 / 33
L23	:	4, 2	$(3y^2 - 1)(35x^4 - 30x^2 + 3) / 16$	1 / 45
L24	:	3, 3	$xy(5y^2 - 3)(5x^2 - 3) / 4$	1 / 49
L25	:	2, 4	$(35y^4 - 30y^2 + 3)(3x^2 - 1) / 16$	1 / 45
L26	:	1, 5	$xy(63y^4 - 70y^2 + 15) / 8$	1 / 33
L27	6	0, 6	$(231y^6 - 315y^4 + 105y^2 - 5) / 16$	1 / 13
L28	7	7, 0	$x(429x^6 - 693x^4 + 315x^2 - 35) / 16$	1 / 15
L29	:	6, 1	$y(231x^6 - 315x^4 + 105x^2 - 5) / 16$	1 / 39
L30	:	5, 2	$x(3y^2 - 1)(63x^4 - 70x^2 + 15) / 16$	1 / 55
L31	:	4, 3	$y(5y^2 - 3)(35x^4 - 30x^2 + 3) / 16$	1 / 63
L32	:	3, 4	$x(35y^4 - 30y^2 + 3)(5x^2 - 3) / 16$	1 / 63
L33	:	2, 5	$y(63y^4 - 70y^2 + 15)(3x^2 - 1) / 16$	1 / 55
L34	:	1, 6	$x(231y^6 - 315y^4 + 105y^2 - 5) / 16$	1 / 39
L35	7	0, 7	$y(429y^6 - 693y^4 + 315y^2 - 35) / 16$	1 / 15
L36	8	8, 0	$(6435x^8 - 12012x^6 + 6930x^4 - 1260x^2 + 35) / 128$	1 / 17
L37	:	7, 1	$xy(429x^6 - 693x^4 + 315x^2 - 35) / 16$	1 / 45
L38	:	6, 2	$(3y^2 - 1)(231x^6 - 315x^4 + 105x^2 - 5) / 32$	1 / 65
L39	:	5, 3	$xy(5y^2 - 3)(63x^4 - 70x^2 + 15) / 16$	1 / 77
L40	:	4, 4	$(35y^4 - 30y^2 + 3)(35x^4 - 30x^2 + 3) / 64$	1 / 81
L41	:	3, 5	$xy(63y^4 - 70y^2 + 15)(5x^2 - 3) / 16$	1 / 77
L42	:	2, 6	$(231y^6 - 315y^4 + 105y^2 - 5)(3x^2 - 1) / 32$	1 / 65
L43	:	1, 7	$xy(429y^6 - 693y^4 + 315y^2 - 35) / 16$	1 / 45
L44	8	0, 8	$(6\,435y^8 - 12\,012y^6 + 6\,930y^4 - 1\,260y^2 + 35) / 128$	1 / 17

© ISO 2005 – All rights reserved
Copyright International Organization for Standardization
Reproduced by IHS under license with ISO
No reproduction or networking permitted without license from IHS
Not for Resale

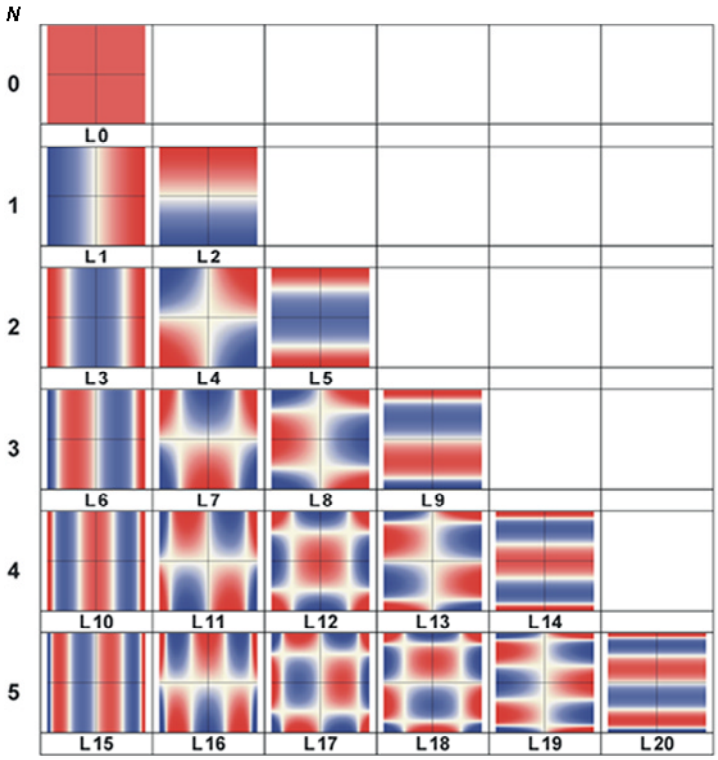

Figure A.2 — Example of visualisation of Legendre (2D) orthogonal set (L0 – L20)

A.3.3 Square areas — "Square-Radial" functions ("S-P")

A.3.3.1 General

Legendre 2D functions have one drawback: The lower order polynomials lack the useful rotationally-symmetric polynomials which are found in the Zernike set, in particular the polynomials up to Z8 (i.e. up to 4th order), including the most desirable power term, i.e. (x^2+y^2).

This inconvenience can be resolved by generating polynomials with explicit rotational symmetry.

The non-rotationally symmetrical nature of the square area makes the polynomials become more complex, from 6th order polynomials upward. However, up to the 4th order inclusive, the polynomials have the same form as the corresponding Zernike polynomials, with only slightly different coefficients.

Also, as the graphs reveal, the underlying rotationally symmetrical features are visible even in the higher order functions.

The definitions are given in A.3.3.2. s^2_{rms} values are given in Table A.4 and Table A.5. An illustration of an alternative set (B0 – B35) for square areas based on the Zernike set (Z0 – Z35) is given in Figure A.3.

A.3.3.2 Definitions

Due to the complex interaction between the square area of definition and the rotationally symmetrical basis of these functions, it is believed there is no simple direct generating formula for the function coefficients or for r.m.s. values of these functions.

No normalizing scheme stands out as being best. We decide to choose the scheme which keeps the coefficient of the basic Zernike function equal to one, in order to highlight the relationship between this set and the Zernike set.

© ISO 2005 – All rights reserved

Copyright International Organization for Standardization
Reproduced by IHS under license with ISO
No reproduction or networking permitted without license from IHS
Not for Resale

This implies that the radius (i.e. half diagonal) of the area should be equal to one, to prevent exponential growth of function amplitude as the order increases. This is not a problem, as any computation routine involves a change of variable (index variable → space variable) which will automatically take this into account.

The alternative would have been an area 2 units square $[-1, +1]^2$, with a large number of $\sqrt{2}$ coefficients to various integer powers, and the relationship between the Zernike set and this alternative set would have been lost.

NOTE The above definition of the area is consistent with ISO 10110.

Indices: $(n + m) = N$: Order of the function;
$(n - m) \geqslant 0$: m is not greater than n;
$(n - m)$ is even.

Area of definition: Centred square, length of sides equal to $\sqrt{2}$.

Polynomial formula: No known formula

Principal term: Zernike function of identical index

Polynomial mean-square value (s^2_{rms}): No known formula

Table A.4 — Square — Polar ("S-P-Z")

Orthogonal on the square (extendible to the rectangle) **Based on polar symmetry** **Expressed as combinations of Zernike functions**				
B	N	n, m	**Formula**	s^2_{rms}
B0	0	0, 0	Z00	1
B1	2	1, 1	Z01	1 / 6
B2	:	1, 1	Z02	1 / 6
B3	2	2, 0	Z03 + (+ Z00) / 3	8 / 45
B4	4	2, 2	Z04	2 / 45
B5	:	2, 2	Z05	1 / 9
B6	:	3, 1	Z06 + (+ 3 Z01) / 5	31 / 525
B7	:	3, 1	Z07 + (+ 3 Z02) / 5	31 / 525
B8	4	4, 0	Z08 + (+ 75 Z03 + 32 Z00) / 105	1072 / 11025
B9	6	3, 3	Z09 + (+ 13 Z06 + 14 Z01) / 31	4 / 155
B10	:	3, 3	Z10 + (– 13 Z07 – 14 Z02) / 31	4 / 155
B11	:	4, 2	Z11 + (+ 9 Z04) / 7	128 / 11025
B12	:	4, 2	Z12 + (+ 3 Z05) / 5	32 / 525
B13	:	5, 1	Z13 + (+ 22 Z09 + 58 Z06 + 41 Z01) / 63	7864 / 218295
B14	:	5, 1	Z14 + (– 22 Z10 + 58 Z07 + 41 Z02) / 63	7864 / 218295
B15	6	6, 0	Z15 + (+ 12495 Z08 + 8925 Z03 + 3071 Z00) / 15477	15094528 / 232387155
B16	8	4, 4	Z16 + (+ 120120 Z15 + 664605 Z08 + 980115 Z03 + 483218 Z00) / 1768890	36224 / 4422225
B17	:	4, 4	Z17	8 / 525

© ISO 2005 – All rights reserved
Copyright International Organization for Standardization
Reproduced by IHS under license with ISO
No reproduction or networking permitted without license from IHS
Not for Resale

Table A.4 *(continued)*

Orthogonal on the square (extendible to the rectangle) **Based on polar symmetry** **Expressed as combinations of Zernike functions**				
B	N	n, m	**Formula**	s^2_{rms}
B18	:	5, 3	Z18 + (+ 22323 Z13 + 64154 Z09 + 41522 Z06 + 34843 Z01) / 41286	13744 / 1300509
B19	:	5, 3	Z19 + (– 22323 Z14 + 64154 Z10 – 41522 Z07 – 34843 Z02) / 41286	13744 / 1300509
B20	:	6, 2	Z20 + (+ 20 Z11 + 21 Z04) / 11	21584 / 3468465
B21	:	6, 2	Z21 + (+ 70 Z12 + 51 Z05) / 105	15692 / 363825
B22	:	7, 1	Z22 + (+ 864087 Z18 + 2026506 Z13 + 1134773 Z09 + 1990834 Z06 + 1212261 Z01) / 1842555	294122552 / 11856841425
B23	:	7, 1	Z23 + (– 864087 Z19 + 2026506 Z14 – 1134773 Z10 + 1990834 Z07 + 1212261 Z02) / 1842555	294122552 / 11856841425
B24	8	8, 0	Z24 + (– 8612340 Z16 + 10975965 Z15 + 6568980 Z08 + 907020 Z03 – 639832 Z00) / 12747735	445621440256 / 9761769292275
B25	10	5, 5	Z25 + (+ 343200 Z22 + 3801861 Z18 + 5694111 Z13 + 7868964 Z09 + 11684564 Z06 + 10254815 Z01) / 13085961	3885824 / 824415543
B26	:	5, 5	Z26 + (+ 343200 Z23 – 3801861 Z19 + 5694111 Z14 – 7868964 Z10 + 11684564 Z07 + 10254815 Z02) / 13085961	3885824 / 824415543
B27	:	6, 4	Z27 + (+ 9556747200 Z24 + 485309083350 Z16 + 104976214413 Z15 + 241581074175 Z08 + 278891981907 Z03 + 125767845785 Z00) / 219329302626	6098940928 / 2302957677573
B28	:	6, 4	Z28 + (+ 5 Z17) / 3	128 / 14553
B29	:	7, 3	Z29 + (+ 10500525 Z25 + 18246063 Z22 + 58262733 Z18 + 44661096 Z13 + 72565827 Z09 + 59713349 Z06 + 43678682 Z01) / 29553513	417760352 / 63392285385
B30	:	7, 3	Z30 + (– 10500525 Z26 – 18246063 Z23 + 58262733 Z19 – 44661096 Z14 + 72565827 Z10 – 59713349 Z07 – 43678682 Z02) / 29553513	417760352 / 63392285385
B31	:	8, 2	Z31 + (+ 1192191 Z20 + 1560570 Z11 + 1327654 Z04) / 578721	756525056 / 189927551385
B32	:	8, 2	Z32 + (+ 1226841 Z21 + 1021890 Z12 + 606094 Z05) / 1682967	7459996672 / 227427745545
B33	:	9, 1	Z33 + (+ 1600891106100 Z29 – 1320930574362 Z25 + 3943425340140 Z22 + 2010790258758 Z18 + 3869204991723 Z13 + 1481222960892 Z09 + 2470347780452 Z06 + 957408066380 Z01) / 3332356832805	296056766869279616 / 16161414123795165225
B34	:	9, 1	Z34 + (– 1600891106100 Z30 – 1320930574362 Z26 + 3943425340140 Z23 – 2010790258758 Z19 + 3869204991723 Z14 – 1481222960892 Z10 + 2470347780452 Z07 + 957408066380 Z02) / 3332356832805	296056766869279616 / 16161414123795165225
B35	10	10, 0	Z35 + (– 1151734265220 Z27 + 737301274281 Z24 – 2706670044780 Z16 + 154349308575 Z15 – 816977558115 Z08 – 1259889678780 Z03 – 608757478628 Z00) / 825304636299	2092531250169856 / 61578454828177287
B36	12	6, 6	Z36 + (+ 379236 Z31 + 2216935 Z20 + 4808345 Z11 + 5491445 Z04) / 2585779	1332224 / 814520385
B37	:	6, 6	Z37 + (– 1189188 Z32 + 7465633 Z21 + 21831635 Z12 + 26931447 Z05) / 50996071	4722176 / 1784862485
B38	:	7, 5	Z38 + (+ 114177559976480 Z33 + 2718028698156711 Z29 + 17511054853329675 Z25 + 4358940067034998 Z22 + 7869806791152003 Z18 + 12417760488627315 Z13 + 11575828368412182 Z09 + 18015128041522780 Z06 + 13756650017852507 Z01) / 6938830473498741	813356273125888 / 381635676042430755
B39	:	7, 5	Z39 + (+ 114177559976480 Z34 – 2718028698156711 Z30 + 17511054853329675 Z26 + 4358940067034998 Z23 – 7869806791152003 Z19 + 12417760488627315 Z14 – 11575828368412182 Z10 + 18015128041522780 Z07 + 13756650017852507 Z02) / 6938830473498741	813356273125888 / 381635676042430755

--`,,`,,,--`--`,,`,`,,`---

© ISO 2005 – All rights reserved

Copyright International Organization for Standardization
Reproduced by IHS under license with ISO
No reproduction or networking permitted without license from IHS

Not for Resale

Table A.4 *(continued)*

Orthogonal on the square (extendible to the rectangle) **Based on polar symmetry** **Expressed as combinations of Zernike functions**				
B	N	n, m	**Formula**	s^2_{rms}
B40	:	8, 4	Z40 + (+ 68800652018384 Z35 + 6092045986115943 Z27 + 1209786609952206 Z24 + 9693088363923120 Z16 + 3548333026828534 Z15 + 5740888340735710 Z08 + 5637669480351546 Z03 + 2374752927284972 Z00) / 2191640396296065	34372402627846144 / 22782101919497595675
B41	:	8, 4	Z41 + (+ 1309 Z28 + 1640 Z17) / 715	1829888 / 289864575
B42	:	9, 3	Z42 + (+ 565343535104700 Z38 + 763706003264490 Z33 + 2565149624175160 Z29 + 1356073133541852 Z25 + 2185857300250140 Z22 + 3853159465260237 Z18 + 3642373821037512 Z13 + 3984711111787388 Z09 + 4033165203174388 Z06 + 2681526736697390 Z01) / 1135839326728535	25268411269096448 / 5684875830276317675
B43	:	9, 3	Z43 + (– 565343535104700 Z39 – 763706003264490 Z34 + 2565149624175160 Z30 – 1356073133541852 Z26 – 2185857300250140 Z23 + 3853159465260237 Z19 – 3642373821037512 Z14 + 3984711111787388 Z10 – 4033165203174388 Z07 – 2681526736697390 Z02) / 1135839326728535	25268411269096448 / 5684875830276317675
B44	:	10, 2	Z44 + (– 170318162 Z36 + 935684607 Z31 + 1286533983 Z20 + 1206708975 Z11 + 781291862 Z04) / 420643223	3194409588224 / 1224032659110261
B45	:	10, 2	Z45 + (– 746613322 Z37 + 1087917831 Z32 + 863622851 Z21 + 383016235 Z12 + 6300234 Z05) / 1412530119	106353538582784 / 4110331280988933
B46	:	11, 1	Z46 + (+ 5481321147735098165 5 Z42 – 80053597227333592698 Z38 + 138326565674454965535 Z33 + 56896102875766473374 Z29 – 211314952678042237854 Z25 + 115516375966780380240 Z22 + 2793334186377137523 Z18 + 8502939649491243987 Z13 – 61335810959613726368 Z09 – 99148881650057560237 Z06 – 103993993393227042614 Z01) / 110971977638848086033	47871904279704287142288128 / 33759623155945149555148479 15
B47	:	11, 1	Z47 + (– 5481321147735098165 5 Z43 – 80053597227333592698 Z39 + 138326565674454965535 Z34 – 56896102875766473374 Z30 – 211314952678042237854 Z26 + 115516375966780380240 Z23 – 2793334186377137523 Z19 + 8502939649491243987 Z14 + 61335810959613726368 Z10 – 99148881650057560237 Z07 – 103993993393227042614 Z02) / 110971977638848086033	47871904279704287142288128 / 33759623155945149555148479 15
B48	12	12, 0	Z48 + (– 80853710242804488990 Z40 + 39068803210909062591 Z35 – 229381305081911332434 Z27 – 6538623897041164656 Z24 – 354429442668777376320 Z16 – 103390075176526996032 Z15 – 192611588458927386735 Z08 – 194559707811599680053 Z03 – 82356423526294057232 Z00) / 42548372864001121845	16755837801383953674649 6 / 62531216179579248719504 25

Copyright International Organization for Standardization
Reproduced by IHS under license with ISO
No reproduction or networking permitted without license from IHS
Not for Resale
© ISO 2005 – All rights reserved

Table A.5 — Square — Polar ("S-P-P")

Orthogonal on the square (extendible to the rectangle)

Based on polar symmetry

Expressed in polar coordinates: $\Sigma\{P_n(r)\cos(m\theta)\}$ or $\Sigma\{P_n(r)\sin(m\theta)\}$; $N = n + m$ (similar to the Zernike set)

B	N	n, m	Formula	s^2_{rms}
B0	0	0, 0	1	1
B1	2	1, 1	$r\cos\theta$	1 / 6
B2	:	1, 1	$r\sin\theta$	1 / 6
B3	2	2, 0	$2r^2 - 2/3$	8 / 45
B4	4	2, 2	$r^2\cos2\theta$	2 / 45
B5	:	2, 2	$r^2\sin2\theta$	1 / 9
B6	:	3, 1	$r(15r^2 - 7)\cos\theta/5$	31 / 525
B7	:	3, 1	$r(15r^2 - 7)\sin\theta/5$	31 / 525
B8	4	4, 0	$2(315r^4 - 240r^2+31)/105$	1072 / 11025
B9	6	3, 3	$r^3\cos3\theta+3r(13r^2 - 4)\cos\theta/31$	4 / 155
B10	:	3, 3	$r^3\sin3\theta+3r(4 - 13r^2)\sin\theta/31$	4 / 155
B11	:	4, 2	$4r^2(7r^2 - 3)\cos2\theta/7$	128 / 11025
B12	:	4, 2	$4r^2(5r^2 - 3)\sin2\theta/5$	32 / 525
B13	:	5, 1	$22r^3\cos3\theta/63+2r(105r^4 - 97r^2+19)\cos\theta/21$	7864 / 218295
B14	:	5, 1	$2r(105r^4 - 97r^2+19)\sin\theta/21 - 22r^3\sin3\theta/63$	7864 / 218295
B15	6	6, 0	$4(77385r^6 - 97335r^4+32151r^2 - 2209)/15477$	15094528 / 232387155
B16	8	4, 4	$r^4\cos4\theta+(1201200r^6+192015r^4 - 292980r^2+23794)/884445$	36224 / 4422225
B17	:	4, 4	$r^4\sin4\theta$	8 / 525
B18	:	5, 3	$5r^3(20643r^2 - 10099)\cos3\theta/20643+r(37205r^4 - 23885r^2+3128)\cos\theta/6881$	13744 / 1300509
B19	:	5, 3	$5r^3(20643r^2 - 10099)\sin3\theta/20643 - r(37205r^4 - 23885r^2+3128)\sin\theta/6881$	13744 / 1300509
B20	:	6, 2	$r^2(165r^4 - 140r^2+27)\cos2\theta/11$	21584 / 3468465
B21	:	6, 2	$r^2(1575r^4 - 1820r^2+471)\sin2\theta/105$	15692 / 363825
B22	:	7, 1	$r^3(864087r^2 - 464315)\cos3\theta/368511+r(64489425r^6 - 90288240r^4+36931080r^2 - 4060109)\cos\theta/1842555$	294122552 / 11856841425
B23	:	7, 1	$r^3(464315 - 864087r^2)\sin3\theta/368511+r(64489425r^6 - 90288240r^4+36931080r^2 - 4060109)\sin\theta/1842555$	294122552 / 11856841425
B24	8	8, 0	$2(446170725r^8 - 782581800r^6+428715540r^4 - 80421480r^2+3396949)/12747735 - 52196r^4\cos4\theta/77259$	445621440256 / 9761769292275
B25	10	5, 5	$r^5\cos5\theta+5r^3(1267287r^2 - 489232)\cos3\theta/4361987+10r(1201200r^6+3634911r^4 - 2297964r^2+259522)\cos\theta/13085961$	3885824 / 824415543
B26	:	5, 5	$r^5\sin5\theta+5r^3(489232 - 1267287r^2)\sin3\theta/4361987+10r(1201200r^6+3634911r^4 - 2297964r^2+259522)\sin\theta/13085961$	3885824 / 824415543
B27	:	6, 4	$2r^4(15666378759r^2 - 7277826545)\cos4\theta/5222126253+10(33448615200r^8+38078984013r^6 - 41984636967r^4+8843857386r^2 - 348126458)/109664651313$	6098940928 / 2302957677573
B28	:	6, 4	$2r^4(9r^2 - 5)\sin4\theta/3$	128 / 14553
B29	:	7, 3	$59325r^5\cos5\theta/166969+r^3(206874591r^4 - 198430575r^2+45016675)\cos3\theta/9851171+5r(127722441r^6 - 129630564r^4+38117757r^2 - 2949796)\cos\theta/29553513$	417760352 / 63392285385

--`,,`,,,-`-`,,`,,`,`,,`---

© ISO 2005 – All rights reserved

Copyright International Organization for Standardization
Reproduced by IHS under license with ISO
No reproduction or networking permitted without license from IHS
Not for Resale

Table A.5 *(continued)*

Orthogonal on the square (extendible to the rectangle)

Based on polar symmetry

Expressed in polar coordinates: $\Sigma\{P_n(r)\cos(m\theta)\}$ or $\Sigma\{P_n(r)\sin(m\theta)\}$; $N = n + m$ (similar to the Zernike set)

B	N	n, m	Formula	s^2_{rms}
B30	:	7, 3	$-59325r^5\sin5\theta/166969+r^3(206874591r^4-198430575r^2+45016675)\sin3\theta/9851171-5r(127722441r^6-129630564r^4+38117757r^2-2949796)\sin\theta/29553513$	417760352 / 63392285385
B31	:	8, 2	$8r^2(4051047r^6-5360355r^4+2140215r^2-248515)\cos2\theta/578721$	756525056 / 189927551385
B32	:	8, 2	$8r^2(11780769r^6-19788615r^4+10066095r^2-1491025)\sin2\theta/1682967$	7459996672 / 227427745545
B33	:	9, 1	$-62901455922r^5\cos5\theta/158683658705+2r^3(1120623774270r^4-1265759396307r^2+314899099562)\cos3\theta/222157122187+2r(41987696093343r^8-79504002628050r^6+5018814643 9788r^4-12065806632342r^2+851241028411)\cos\theta/666471366561$	296056766869279616 / 16161414123795165225
B34	:	9, 1	$-62901455922r^5\sin5\theta/158683658705-2r^3(1120623774270r^4-126575939630 7r^2+314899099562)\sin3\theta/222157122187+2r(41987696093343r^8-79504002628050r^6+50188146439 788r^4-12065806632342r^2+851241028411)\sin\theta/666471366561$	296056766869279616 / 16161414123795165225
B35	10	10, 0	$120r^4(8477781337-19195571087r^2)\cos4\theta/275101545433+4(51994192086837r^{10}-117082707917175r^8+905088510 24900r^6-29122300885860r^4+3561847824345r^2-102049507139)/825304636299$	2092531250169856 / 61578454828177287
B36	12	6, 6	$r^6\cos6\theta+r^2(21237216r^6-6565755r^4-2351160r^2+575660)\cos2\theta/2585779$	1332224 / 814520385
B37	:	6, 6	$r^6\sin6\theta-3r^2(22198176r^6-78949745r^4+44445800r^2-6040740)\sin2\theta/50996071$	4722176 / 1784862485
B38	:	7, 5	$7r^5(2312943491166247r^2-1148663237507751)\cos5\theta/2312943491166247+21r^3(906009566052237r^4-669711539507005r^2+115506161672560)\cos3\theta/2312943491166247+10r(479545751901216r^8+4019772851760351r^6-3779383718025531r^4+964993555783390r^2-62839902252290)\cos\theta/2312943491166247$	813356273125888 / 381635676042430755
B39	:	7, 5	$7r^5(2312943491166247r^2-1148663237507751)\sin5\theta/2312943491166247-21r^3(906009566052237r^4-669711539507005r^2+115506161672560)\sin3\theta/2312943491166247+10r(479545751901216r^8+4019772851760351r^6-3779383718025531r^4+964993555783390r^2-62839902252290)\sin\theta/2312943491166247$	813356273125888 / 381635676042430755
B40	:	8, 4	$4r^4(5113827591357485r^4-4624718393978256r^2+1008955364815365)\cos4\theta/730546798765355+4(1444813692386064r^{10}+3445054327089375r^8-4989591643870260r^6+1868999767616345r^4-226808950021780r^2+5885393231202)/730546798765355$	34372402627846144 / 22782101919497595675
B41	:	8, 4	$4r^4(5005r^4-5544r^2+1455)\sin4\theta/715$	1829888 / 289864575
B42	:	9, 3	$84r^5(4282905568975r^2-2203450299877)\cos5\theta/103258120611685+4r^3(4770525172259847r^6-6847643239135776r^4+3078721895377128r^2-424660852103633)\cos3\theta/227167865345707+12r(1603782606855429r^8-2288877923421705r^6+1094176014681827r^4-197593857188203r^2+10290310146384)\cos\theta/227167865345707$	25268411269096448 / 5684875830276317675
B43	:	9, 3	$84r^5(2203450299877-4282905568975r^2)\sin5\theta/103258120611685+4r^3(4770525172259847r^6-6847643239135776r^4+3078721895377128r^2-424660852103633)\sin3\theta/227167865345707-12r(1603782606855429r^8-2288877923421705r^6+1094176014681827r^4-197593857188203r^2+10290310146384)\sin\theta/227167865345707$	25268411269096448 / 5684875830276317675
B44	:	10, 2	$10r^2(8833507683r^8-15960584640r^6+9772127967r^4-2365281856r^2+183317111)\cos2\theta/420643223-24331166r^6\cos6\theta/60091889$	3194409588224 / 1224032659110261
B45	:	10, 2	$10r^2(9887710833r^8-21699726048r^6+16399520683r^4-4940651296r^2+478258737)\sin2\theta/470843373-8204542r^6\sin6\theta/15522309$	106353538582784 / 4110331280988933

© ISO 2005 – All rights reserved
Copyright International Organization for Standardization
Reproduced by IHS under license with ISO
No reproduction or networking permitted without license from IHS
Not for Resale

Table A.5 *(continued)*

Orthogonal on the square (extendible to the rectangle) **Based on polar symmetry** **Expressed in polar coordinates**: $\Sigma\{P_n(r)\cos(m\theta)\}$ or $\Sigma\{P_n(r)\sin(m\theta)\}$; $N = n + m$ (similar to the Zernike set)				
B	N	n, m	**Formula**	s^2_{rms}
B46	:	11, 1	$2r^5(6404919778237126627 - 13342266204555598783r^2)\cos5\theta/5284379887564194573+2r^3(328879268864105889930r^6 - 572414383414562069799r^4+2901764849843388971 55r^2 - 4284373917817 6941130)\cos3\theta/1585313966269258371 9+2r(8544842278191302624541r^{10} - 203992574249945437906 95r^8+1752272109915641856003 0r^6 - 665694788460521596511 0r^4+1069746603645182483335r^2 - 52742265078762233277)\cos\theta/3699065921294936201 1$	47871904279704287142288128 / 33759623155945149555148479 15
B47	:	11, 1	$2r^5(6404919778237126627 - 13342266204555598783r^2)\sin5\theta/5284379887564194573 - 2r^3(328879268864105889930r^6 - 572414383414562069799r^4+2901764849843388971 55r^2 - 4284373917817 6941130)\sin3\theta/1585313966269258371 9+2r(8544842278191302624541r^{10} - 203992574249945437906 95r^8+1752272109915641856003 0r^6 - 665694788460521596511 0r^4+1069746603645182483335r^2 - 52742265078762233277)\sin\theta/3699065921294936201 1$	47871904279704287142288128 / 33759623155945149555148479 15
B48	12	12, 0	$4(98286741315842591461 95r^{12} - 27024687792465506495352r^{10}+ 27239081206484485713375r^8 - 12688782692839396629360r^6+ 27558561255995271930 75r^4 - 2395814682519777346 80r^2+ 4980679189739031679) / 42548372864001121845 - 24r^4(4491872791266916055r^4 - 4007079364496667744r^2+ 833985259724777875)\cos4\theta/2026112993523862945$	16755837801383953674649 6 / 62531216179579248719504 25

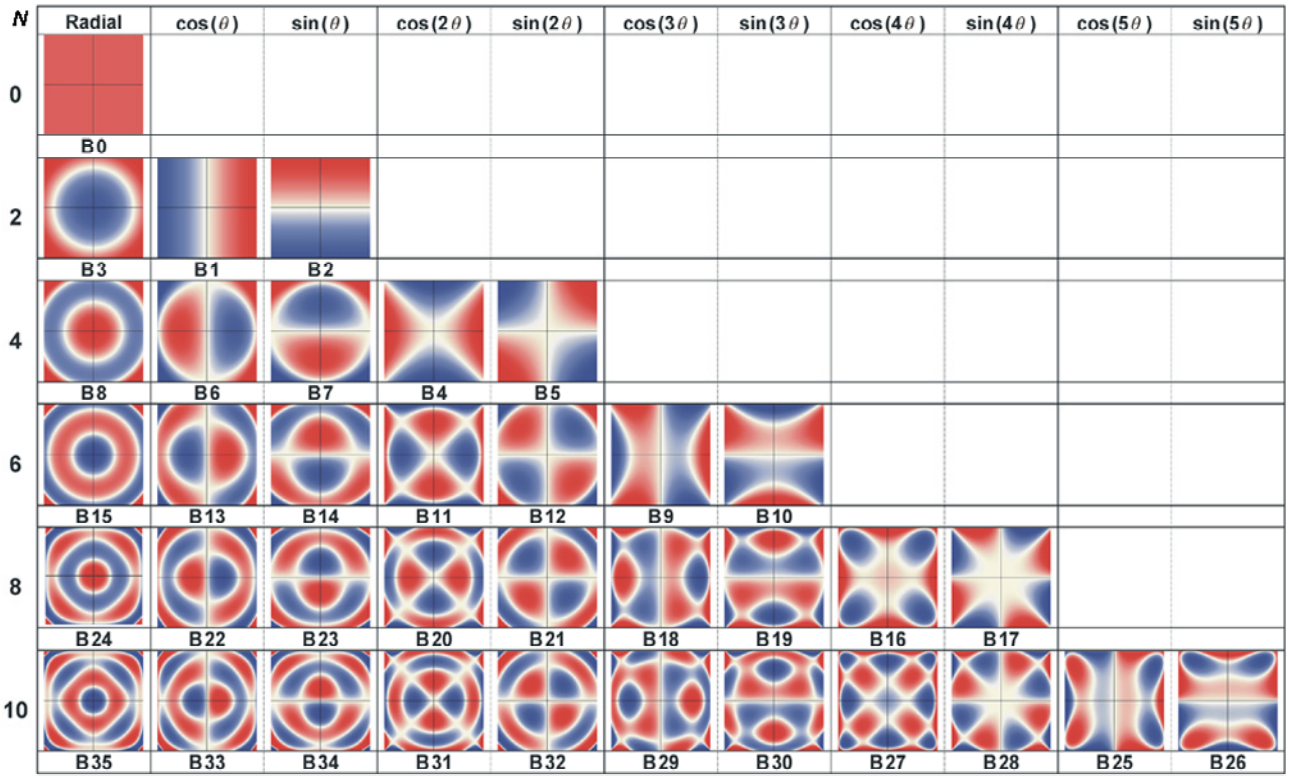

Figure A.3 — Example of visualisation of alternative set (B0 – B35) for square areas based on Zernike set (Z0 – Z35)

© ISO 2005 – All rights reserved

Copyright International Organization for Standardization
Reproduced by IHS under license with ISO
No reproduction or networking permitted without license from IHS
Not for Resale

Annex B
(informative)

Orthogonal functions on "unusual areas"

B.1 General

This Annex suggests how to compute orthogonal polynomials, given certain desired characteristics, over an arbitrarily shaped area, including a weight function if desired. Mathematically, this is not a new method but it does not seem to be applied in the optics world. The term orthogonal *function*, and not *polynomial*, is used in this text as this method applies to absolutely any base of functions. This could include, e.g. $R \times (1 - \cos\theta)$, to accurately model defocus.

This annex gives a few examples of orthogonal polynomials, without showing the details of the computation. This computation can be very simple using matrix notation, enabling the generation of the polynomials one after the other, in a deterministic way (no iterations or approximations).

B.2 Preliminary considerations

Decide if the functions/polynomials generated will be used for storage of data, or for analysis of data.

a) Storage

In this case, it is essential that the functions be orthogonal, or that their possible lack of orthogonality be taken into account, otherwise the reconstruction will be erroneous, possibly only by a small amount.

This is often the case with discrete pupils (such as given by digital interferometers, etc.). In this case, generate a specific set of orthogonal functions for each pupil.

b) Analysis

The lack of orthogonality will only, possibly, affect the value of the amplitudes of the functions that we compute.

If the functions are "almost" orthogonal (e.g. Zernike on a discrete pupil), the error will be small. For Z3, "curvature", e.g. the error is in $1/n2$; for higher order deformations, it might get worse.

B.3 General method and definitions

Use x and y as general coordinates, even if not in rectangular coordinates.

Generate the series $\{f_0(x,y), f_1(x,y), \ldots f_n(x,y)\}$.

B.3.1
base area
"pupil"

NOTE The weight function (B.3.2) can participate in this definition.

© ISO 2005 – All rights reserved
Copyright International Organization for Standardization
Reproduced by IHS under license with ISO
No reproduction or networking permitted without license from IHS
Not for Resale

B.3.2
weight function
$w(x,y)$
amplitude of the wavefront over the pupil

B.3.3
correlation of two functions
$f_1(x,y)$
$f_2(x,y)$

Correlation: $C(f_1,f_2) = \iint\left[\left(\left\{w(x,y)\times f_1(x,y)\right\}\times\left\{w(x,y)\times f_2(x,y)\right\}\right)\times \mathrm{d}^2S\right]$

In short: $C(1,2) = C(f_1,f_2)$.

B.4 Generation

B.4.1 Initial conditions

In optics, for obvious reasons, it is preferable to start the function series with {1, x, y}, or even {1, x, y, r^2}

NOTE ISO 10110-5 and ISO 10110-14 define the "centre" of a pupil in such a way that the three first functions are always orthogonal. {r^2} can never be orthogonal with {1}, because it is always positive, like {1}.

B.4.2 Property — Examples

B.4.2.1 Example 1 — Zernike functions (polynomials)

Zn should be of the form: {r^{2n} ($r\cos\phi)^p$} = {r^{2n+p} cos $\phi\, p$}, where n and p are integers. In practice, the cosine term is expanded and written: {r^{2n+p} cos $p\ \phi$}. This *considerably* simplifies computation. Zernike is one of the easiest set of polynomials to generate.

B.4.2.2 Example 2 — "Radial-square" functions

Consider as an example:

Z6 = {$(3r^2 - 2)\ r\cos\phi$}

which can also be written as

$Z6$ = {$(3r^3\cos\phi - 2r\cos\phi$} = {$(3r^2x - 2x$}

The "$2x$" term is only there to "correct" the average tilt of the *basic term*, {r^3 cos ϕ} = $r^2\,x$ (the coefficient 3 is there for overall normalization).

On a square pupil, the average tilt of the basic term will probably be different. The "Radial-square" functions are defined as being similar to Zernike, in their basic term, but with different "correction terms".

There is a great drawback with any "square" set of functions. Because of the 4-symmetry of the square pupil, there will *always* be correlation between {cos(4ϕ)} = $x^4 - 6x^2y^2+y^4$ and any rotationally symmetric term. But the pupil (i.e. amplitude) function has a role in the wavefront propagation and diffraction, so it is not strictly correct to talk of rotationally symmetric functions on a non-rotationally symmetric pupil.

This means that, contrary to the circular pupil (Zernike), it will not be possible to generate the rotationally symmetrical functions first, and then the cos(ϕ) terms, then the cos(2ϕ) terms, etc. Therefore it is necessary to generate the functions in a different order, e.g. like the classical Zernike functions.

© ISO 2005 – All rights reserved

Copyright International Organization for Standardization
Reproduced by IHS under license with ISO
No reproduction or networking permitted without license from IHS
Not for Resale

B.4.2.3 Example 3 — "Square" functions

Here, simply write that the basic term will be of the form {$x^p\ y^q$}, with correction terms in the same form, with pairs of indices "smaller" than (p,q), and of the same parity (this last property is sufficient, as the symmetric square area insures that different parity exponents will cancel upon integration over the pupil).

The basic series is obtained: {1, x, y, x^2, xy, y^2, x^3, x^2y, xy^2, y^3, x^4, x^3y, etc.}.

Notice that each order (p+q) comprises (p+q+1) functions, the same as for Zernike: for order 4 in r, {Z8; Z11; Z12; Z16; Z17}; etc.

B.4.3 Generation of the set

For each polynomial, write that it has zero correlation with all the previously generated polynomials. This gives as many relations to compute the correction terms that accompany the basic term. If the basic terms are chosen properly (which simply means that they are mutually non-correlated), the generation is straightforward.

B.5 Discrete (i.e."real") areas

Discrete areas are areas in their own right. Everything said above applies to them, without any change.

B.6 Matrix computation

Using matrix computations enables easy computation of a whole set of orthogonal functions, based on a set of *basic terms*, using lower-numbered functions as correcting functions. Because the computation of the mutual correlation of single basic terms is very quick, this method is very useful, and compact.

© ISO 2005 – All rights reserved
Copyright International Organization for Standardization
Reproduced by IHS under license with ISO
No reproduction or networking permitted without license from IHS
Not for Resale

Bibliography

[1] ISO 10110-5:1996, *Optics and optical instruments — Preparation of drawings for optical elements and systems — Part 5: Surface form tolerances*

[2] ISO 10110-14:2003, *Optics and optical instruments — Preparation of drawings for optical elements and systems — Part 14: Wavefront deformation tolerance*

[3] ISO/TR 14999-1:2004, *Optics and photonics — Interferometric measurement of optical elements and optical systems — Part 1: Terms, definitions and fundamental relationships*

[4] YODER, P.R., *Opto-Mechanical Systems Design*, Marcel Dekker, New York, 1986

[5] MALACARA, D., ed. *Optical shop testing*, Wiley, New York, 1991

[6] CREATH, K., *Phase-measurement interferometry techniques*, Progress in Optics XXVI, E.Wolf, Elsevier Science publishers B.V., 1988

[7] SCHWIDER, J., *Advanced evaluation techniques in interferometry*. Progress in Optics XXVI, E.Wolf, Elsevier Science publishers B.V., 1988

[8] SCHWIDER, J., BUROW, R., ELSSNER, K., GRZANNA, J., SPOLACZYK, R., MERKEL, K., *Appl. Opt.*, **22**, 1983, p. 3421

[9] TAKEDA, M., INA, H., KOBAYASHI, S., *J. Opt. Soc. Am.*, **72**, 1982, p. 156

[10] KREIS, Th., *J. Opt. Soc. Am.*, **A3**, 1986, p. 847

[11] WOMACK, K.H., *Opt. Eng.* **23**, 1984, p. 391

[12] WOMACK, K.H., *Opt. Eng.*, **23**, 1984, p. 396

[13] BORN, M., WOLF, E., *Principles of Optics*, Pergamon Press, 1980

[14] ABRAMOWITZ, M., and STEGUN, I. A., *Handbook of Mathematical Functions with Formulas, Graphs, and Mathematical Tables*. 9th ed., New York: Dover

[15] BRAY, M., *Orthogonal polynomials: a set for square areas, Optical Fabrication, Testing, and Metrology*. SPIE Vol. 5252, Saint-Étienne, 2003

© ISO 2005 – All rights reserved

Copyright International Organization for Standardization
Reproduced by IHS under license with ISO
No reproduction or networking permitted without license from IHS
Not for Resale

ICS 37.020

Price based on 59 pages

© ISO 2005 – All rights reserved
Copyright International Organization for Standardization
Reproduced by IHS under license with ISO
No reproduction or networking permitted without license from IHS
Not for Resale